

# An efficient Haar wavelet method for the coupled non-linear transient PDE-ODEs system with discontinuous coefficients

B.V. Rathish Kumar\* · Meena Pargaei

the date of receipt and acceptance should be inserted later

**Abstract** In this work, Haar wavelet method for the coupled non-linear transient PDE-ODEs system with Neumann boundary condition has been proposed. The capability of the method in handling multiple jump discontinuities in the coefficients and parameters of the transient and coupled PDE-ODEs system is brought out through a series of 1D/2D/3D test problems. The method is easy to implement, computationally efficient and compare well with conventional methods like finite element method. Convergence analysis of the method has been carried out and apriori error is found to be exponential order i.e.  $\|u - u_H\|_X \sim o(2^{-j})$ . ILU-GMRES is found to better accelerate the numerical solution convergence than other Krylov solvers for the class of transient non-linear PDE-ODE system.

**Keywords** Non-linear coupled PDE-ODEs system · Haar wavelet method · Convergence analysis · Jump discontinuity

## 1 Introduction

Study of coupled PDE-ODEs systems has been an active research theme as such models arise in different fields of physical science, engineering, biology and economics. For instance such models are encountered while dealing with problems related to electro-magnetic coupling, coupling of chemical reaction and transport, mechanical coupling, propagation of electric waves in cardiac tissue etc. J. Daafouz et al. Daafouz et al. (2014) model for a boost converter connected to a load via a transmission line, coupled the partial differential equation describing telegraph with the ODE representing the action of the converter. In Göktepe and Kuhl (2010), E. Sabine presented the mathematical model of mitochondrial swelling phenomena via coupled PDE-ODE system. Such PDE-ODE coupled systems frequently arise in the field of cardiac electrophysiology Plonsey (1988); Keener and Sneyd (1998); Sepulveda et al. (1989). Such PDE-ODE coupled systems are not easily solvable especially when they are non-linear and in addition they have discontinuities or sharp variations either in field variables or coefficients or parameters appearing in the governing mathematical model. This is especially the case in mathematical models representing the cardiac electrical activity in ischemic cardiac tissue. Such discontinuities are also encountered in solid mechanics while dealing with fractures, cracks, inclusions and voids. In fluid mechanics such sharp variations in field variables arise when dealing with shock waves, boundary layers etc.

Several specialized numerical methods based on different operator discretization procedures such as finite differences, finite elements, spectral elements, finite volume etc. have been used to solve such coupled systems with discontinuities or sharp variations. M. Vynnycky and Sarah L. Mitchell Vynnycky and Mitchell (2013) proposed Keller box based finite difference method for parabolic PDE with discontinuous boundary conditions. Several finite element method based adaptive methods have been proposed to deal with jumps, kinks or sharp

---

B.V. Rathish Kumar\*  
Department of Mathematics and Statistics, Indian Institute of Technology, Kanpur, India  
E-mail: drbvrk11@gmail.com\*

Meena Pargaei  
Department of Mathematics and Statistics, Indian Institute of Technology, Kanpur, India  
Department of Mathematics, G.P.G.C. Champawat, Uttarakhand, India  
E-mail: meenamenu15@gmail.com

variations in PDE model. Andreas Bomto et al. in Bonito et al. (2013) proposed adaptive finite element method for elliptic problems with discontinuous coefficients for dealing with diffusion through porous media, or rough surfaces, electromagnetic field propagation on heterogeneous media using distortion theory. C. Bernardi and R. Verfürth in Bernardi and Verfürth (2000) derived a priori and a posteriori errors for adaptive finite element method for elliptic equations with non-smooth coefficients for modeling multilayer fluids with different viscosities. In Bonito and Devaud (2015), Andrea Bonito and Denis Devaud introduced the adaptive finite element method for Stokes problem with discontinuities viscosity. There are also meshfree approximation techniques which provide greater flexibility. C. Armando Duarte and J.T. Oden Duarte and Oden (1996) implemented h-p cloud method, fully exploiting the h, p and h-p adaptivity, devoid of conventional finite element grids on Poisson problems and 3-D elasticity problem. However these methods are not only limited by their adaptivity approach but may turn out to be very costly especially when dealing with the problems with evolving and moving features. In Fries and Belytschko (2010), generalized or extended finite element method has been discussed especially to effectively handle the jumps and singularities but this again gets quite sensitive to indicator function choice and are computationally costly.

Recently, wavelet methods are getting much attention, due to their inherent adaptability to the complexities such as discontinuities, sharp variations etc. in solving the mathematical models from science and engineering. Its properties such as orthogonality, compact support, arbitrary regularity and high order vanishing moments are very attractive. Wavelet based Galerkin and collocation methods have been used to solve integral equations, ODEs, PDEs, fractional differential equations Aziz et al. (2013a, 2010b); Šarler et al. (2011); Aziz et al. (2013b); Aziz and Fayyaz (2013); Aziz et al. (2010a, 2011, 2012); Comincioli et al. (2000); Wu (2009). In Paolucci et al. (2014) parallel wavelet adaptive method has been used in the domain decomposition framework to solve the compressible reacting flow with the shock wave in air. Oleg V. Vasilyev et al. Vasilyev et al. (2004) have developed discontinuous interpolating wavelets for handling multiphase problems with discontinuities across the phase boundaries. Kai Schneider and Oleg V. Vasilyev Schneider and Vasilyev (2010) demonstrated the ability of adaptive wavelet basis in capturing coherent vortex structures in turbulent flows and thereby zoomed into their space-scale structure. They also present a hierarchy of wavelet-based turbulence models for carrying out complex industrial flow simulations. In Kestler et al. (2016) Sebastian Kestler et al. have introduced a space-time adaptive wavelet Galerkin method for time periodic PDEs. In all these studies authors have focused on using either Daubechies class of continuous wavelets or second generation wavelets. Simplest of all the wavelets and easy to implement in a finite domain is the Haar wavelet.

Haar wavelets are piecewise constant functions which are orthogonal and have compact support. They also have scaling property. The ease of using a Haar wavelet has made it very popular in signal processing and image processing. Because of the discontinuity of Haar wavelets, their derivatives does not exist and hence cannot be directly used in approximating solution of a differential equation. Chen and Hsiao Chen and Hsiao (1997) have proposed the idea that the highest order derivative of the differential equation can be expanded into the Haar series and not the field variable function. Then on integration one can obtain lower order derivatives and the function too.

Haar wavelet method has been used to solve the linear and non-linear differential equations and the eigenvalue problems Bujurke et al. (2008); Lepik (2007); Hariharan and Kannan (2010); Singh and Kumar (2017); Shi and Cao (2012). Largely these attempts are confined to 1D studies and this is specially the case with transient PDEs. Further no attempt has been made to test Haar wavelet capability in handling complexities like discontinuities, sharp variations etc. In this work, we propose the Haar wavelet method for the solution of coupled PDE-ODEs system with Neumann boundary condition and having discontinuities in either in source/coefficient function or in any parameter of the model. We will show the power of method in handling problem with multiple discontinuities like those which occur in cardiac electrophysiological models. We easily extend the method to higher dimensions and also to identify the desired linear solver and the influence of preconditioning in convergence acceleration. We also theoretically carry out the error analysis and show that the convergence is of exponential order i.e.  $o(2^{-j})$ . We compare the results against those from finite element method both for quality and computational complexity. The paper is organized as follows:

In section 2, we introduce Haar wavelet function, its properties and Haar integrating functions. In the next section, one and two dimensional Haar wavelet method for non-linear PDE-ODEs system will be developed. Convergence analysis of the proposed method is presented in section 4. Numerical results and discussion for the several problems with different types of discontinuities are provided in section 5. Three dimensional Haar wavelet method is discussed in the next section and its convergence analysis has been established. Further the proposed method has been successfully demonstrated for few practical problems, with discontinuity from cardiac electrophysiology in ischemic cardiac tissue.

## 2 Haar wavelets

Let us consider the interval  $x \in [A, B]$ ,  $A, B$  are finite real numbers. Define  $M = 2^J$ ,  $J$  is the maximum level of resolution. This interval  $[A, B]$  is equally divided into  $2M$  subintervals such that the length of each subinterval is  $\Delta x = (B - A)/2M$ . Now, define the dilation and translation parameter  $j = 0, 1, \dots, J$  and  $k = 0, 1, \dots, m - 1$  respectively, where,  $m = 2^j$ . The wavelet number is given by  $i = m + k + 1$ . Family of haar wavelets is defined as follows:

For  $i = 1$

$$h_i(x) = \begin{cases} 1 & \text{when } A \leq x < B \\ 0 & \text{otherwise.} \end{cases}$$

For  $i \geq 2$

$$h_i(x) = \begin{cases} 1 & \text{when } \beta_1(i) \leq x < \beta_2(i) \\ -1 & \text{when } \beta_2(i) \leq x < \beta_3(i) \\ 0 & \text{otherwise,} \end{cases} \quad (1)$$

where,

$$\begin{aligned} \beta_1(i) &= A + 2k\zeta\Delta x, & \beta_2(i) &= A + (2k + 1)\zeta\Delta x, \\ \beta_3(i) &= A + 2(k + 1)\zeta\Delta x, & \zeta &= M/m. \end{aligned}$$

Haar wavelets are orthogonal, since

$$\int_A^B h_p(x)h_q(x)dx = \begin{cases} 2^{-q}(B - A) & \text{when } p = q \\ 0 & \text{when } p \neq q. \end{cases}$$

For the solution of differential equation, we have to compute the integral

$$p_{\alpha,i}(x) = \int \cdots \int_A^B h_i(t)dt^\alpha = \frac{1}{(\alpha - 1)!} \int_A^x (x - t)^{(\alpha-1)} h_i(t)dt, \quad (2)$$

where  $\alpha = 1, 2, \dots, n$  and  $i = 1, 2, \dots, 2M$ .

For the case,  $\alpha = 0, p_{0,i}(x) = h_i(x)$ .

This integral is calculated with the help of equation (1), defined as

$$p_{\alpha,i}(x) = \begin{cases} 0 & \text{when } x < \beta_1(i) \\ \frac{1}{\alpha!}(x - \beta_1(i))^\alpha & \text{when } \beta_1(i) \leq x < \beta_2(i) \\ \frac{1}{\alpha!}[(x - \beta_1(i))^\alpha - 2(x - \beta_2(i))^\alpha] & \text{when } \beta_2(i) \leq x < \beta_3(i) \\ \frac{1}{\alpha!}[(x - \beta_1(i))^\alpha - 2(x - \beta_2(i))^\alpha + (x - \beta_3(i))^\alpha] & \text{when } x > \beta_3(i). \end{cases} \quad (3)$$

When  $\alpha = 1, 2$ ,

$$p_{1,i}(B) = \begin{cases} (B - A) & \text{when } i = 1 \\ 0 & \text{otherwise.} \end{cases} \quad (4)$$

$$p_{2,i}(B) = \begin{cases} (B - A)^2/2 & \text{when } i = 1 \\ (B - A)^2/4m^2 & \text{otherwise.} \end{cases}$$

For the grid points  $x_k = A + kh, k = 0, 1, \dots, 2M$ ,  $h = \Delta x$ , collocation points are as follows:

$$y_k = \frac{x_{k-1} + x_k}{2}, k = 1, 2, \dots, 2M. \quad (5)$$

After this discretization, we define Haar matrix  $H$ , and Haar Integral matrices  $P_1, P_2$  of size  $2M \times 2M$  as  $H(i, k) = h_i(y_k), P_1(i, k) = p_{1,i}(y_k), P_2(i, k) = p_{2,i}(y_k)$ .

## 2.1 Function approximation

Any function  $f(x) \in L^2[0, 1)$  can be approximated in terms of the Haar wavelet series as

$$f(x) = \sum_{i=1}^{\infty} \alpha_i h_i(x),$$

where the wavelet coefficients  $\alpha_i$  are obtained by

$$\alpha_i = 2^j \int_0^1 f(x) h_i(x) dx.$$

Since only the finite number of terms are taken for the computational purpose therefore, the function approximation  $f$  is given by

$$f(x) = \sum_{i=1}^{2M} \alpha_i h_i(x).$$

where,  $M = 2^J$

## 2.2 Functions consisting the coefficient having jump discontinuities

Let us consider the domain  $[0, 1]$  and a function  $f(x)$  defined on this domain given by

$$f(x) = k(-x^3 + 1.1x^2 - 0.1x) \quad (6)$$

where,  $k$  is a parameter.

Now, if the parameter  $k$  of the above function  $f(x)$  is discontinuities at one or multiple places of the domain, as given in Fig. 1a ( $k = 1.5$  if  $0.46 < x < 0.5$ ,  $k = 1$  otherwise) and Fig. 2a ( $k = 4$  if  $0.2305 < x < 0.2383$ ,  $k = 2$  if  $0.8242 < x < 0.8302$ ,  $k = 1$  otherwise), the corresponding function  $f(x)$  will also be discontinuous, drawn in Fig. 1b, 1c, 1d 2b, 2c, and, 2d respectively.

## 3 Mathematical Model

Let  $\Omega \subset R^n$  then a general non-linear parabolic reaction-diffusion equation coupled with the system of ODEs, is given as follows:

$$\begin{aligned} \epsilon \frac{\partial v}{\partial t} - \text{div}(D(x)\nabla v) + f(v, w) &= 0 & x \in \Omega, 0 \leq t \leq T \\ \frac{\partial w_i}{\partial t} - g_i(v, w) &= 0, & x \in \Omega, 0 \leq t \leq T \\ v(x, 0) = v_0(x, 0), \quad w_i(x, 0) = w_{i,0}(x, 0), & & x \in \Omega \\ n^T D(x)\nabla v &= 0, & x \in \partial\Omega, 0 \leq t \leq T, \end{aligned}$$

where,  $i = 1, 2, \dots, d$  and  $D(x)$  is the diffusion tensor.

Remark: For existence-uniqueness and stability of such coupled system one may refer to Bourgault et al. (2006); Veneroni (2009).

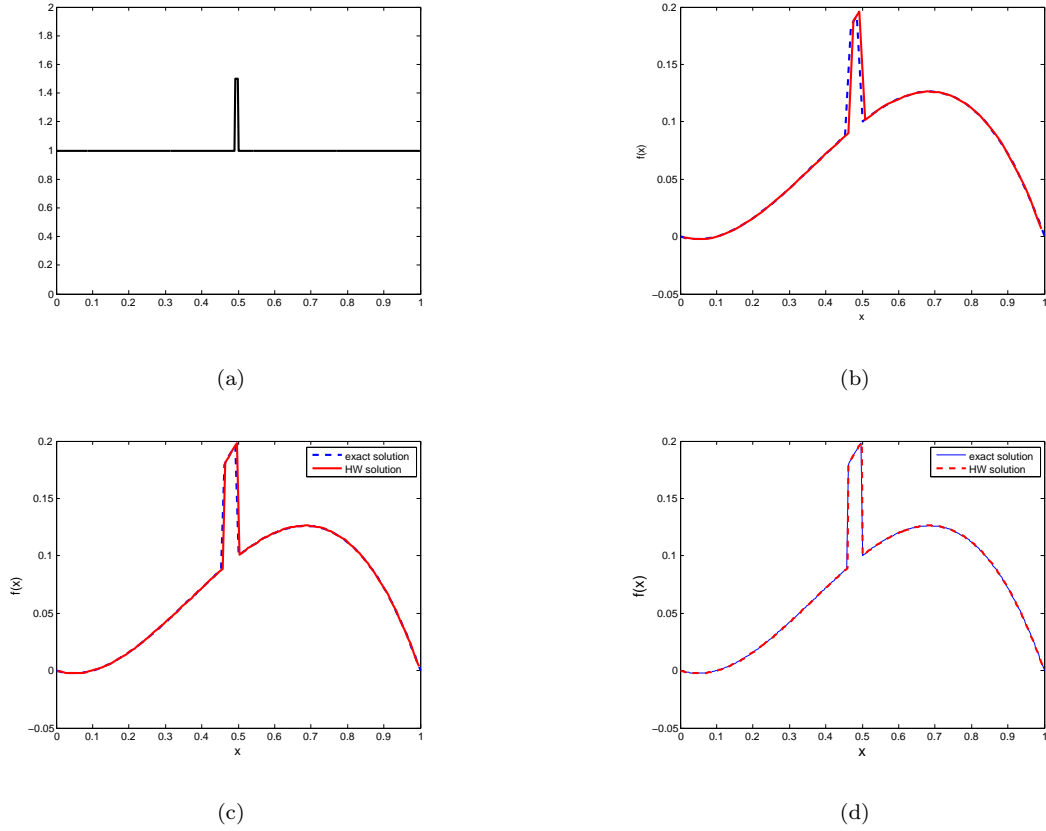


Fig. 1: (a) Value parameter  $k$ , (b) Corresponding function  $f(x)$ ,  $J = 5$ , (c)  $J = 6$ , (d)  $J = 7$ .

### 3.1 Haar wavelet algorithm for the coupled non-linear PDE-ODEs system

Consider the three dimensional non-linear parabolic reaction-diffusion equation coupled with a system of ODEs given as follows:

$$\epsilon(x, y, z) \frac{\partial v}{\partial t} - \text{div}(D(x, y, z) \nabla v) + f(v, w) = 0, \quad 0 \leq x, y, z \leq 1, 0 \leq t \leq T \quad (7)$$

$$\frac{\partial w}{\partial t} - g(v, w) = 0, \quad 0 \leq x, y, z \leq 1, 0 \leq t \leq T \quad (8)$$

$$v(x, y, z, 0) = v_0(x, y, z, 0), \quad w(x, y, z, 0) = w_0(x, y, z, 0), \quad 0 \leq x, y, z \leq 1 \quad (9)$$

with Neumann boundary conditions in  $v$ .

Let us write  $\frac{\partial^7 v}{\partial t \partial x^2 \partial y^2 \partial z^2}(x, y, z, t)$  in terms of the Haar wavelet as follows:

$$\frac{\partial^7 v}{\partial t \partial x^2 \partial y^2 \partial z^2}(x, y, z, t) = \sum_{i,j,k=1}^{2M} \alpha_{i,j,k} h_i(x) h_j(y) h_k(z), \quad t \in [t_s, t_{s+1}) \quad (10)$$

$$\frac{\partial w}{\partial t}(x, y, z, t) = \sum_{l,m,n=1}^{2M} \beta_{l,m,n} h_l(x) h_m(y) h_n(z), \quad t \in [t_s, t_{s+1}). \quad (11)$$

Integrating equation (10) w.r.t  $t$  from  $t_s$  to  $t$ , we will get

$$\frac{\partial^6 v}{\partial x^2 \partial y^2 \partial z^2}(x, y, z, t) = (t - t_s) \sum_{i,j,k=1}^{2M} \alpha_{i,j,k} h_i(x) h_j(y) h_k(z) + \frac{\partial^6 v}{\partial x^2 \partial y^2 \partial z^2}(x, y, z, t_s), \quad t \in [t_s, t_{s+1}). \quad (12)$$

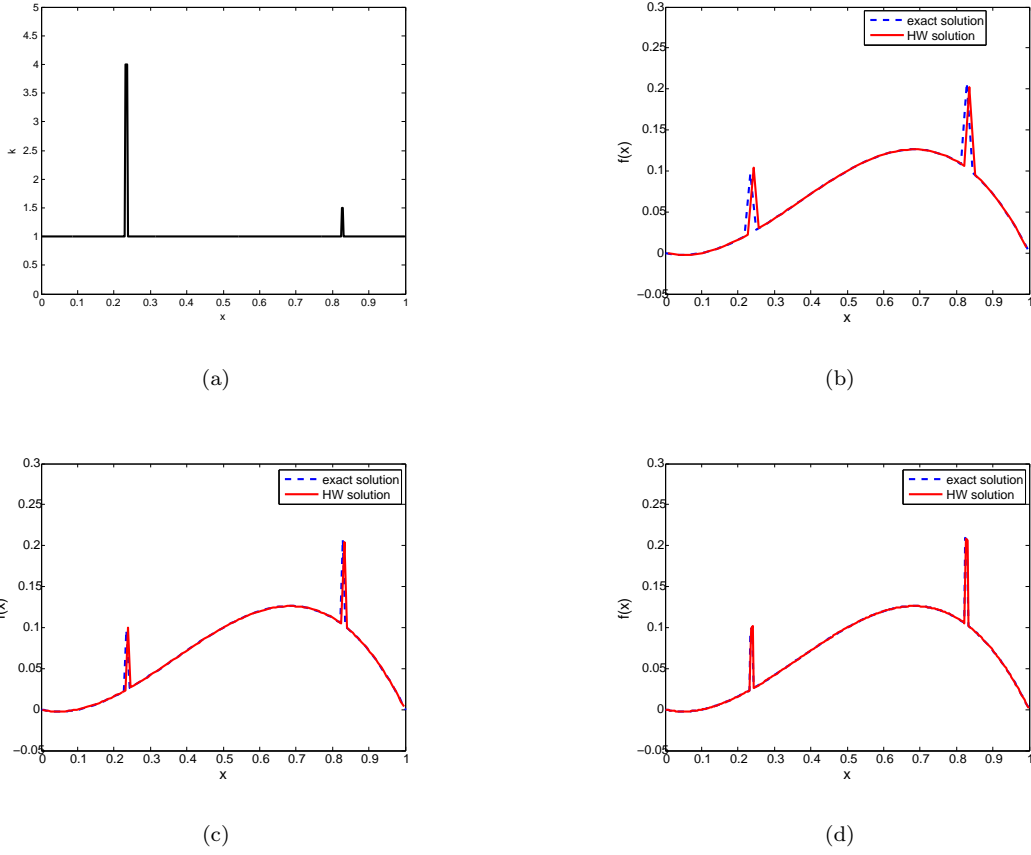


Fig. 2: (a) Value parameter  $k$ , (b) Corresponding function  $f(x)$   $J = 5$ , (c)  $J = 6$ , (d)  $J = 7$ .

Now, Integrate equation (12) twice w.r.t  $x$  from 0 to  $x$  also using the boundary conditions, we will obtain the following

$$\begin{aligned} \frac{\partial^4 v}{\partial y^2 \partial z^2}(x, y, z, t) &= (t - t_s) \sum_{i,j,k=1}^{2M} \alpha_{i,j,k} P_{2,i}(x) h_j(y) h_k(z) + \frac{\partial^4 v}{\partial y^2 \partial z^2}(x, y, z, t_s) - \frac{\partial^4 v}{\partial y^2 \partial z^2}(0, y, z, t_s) \\ &+ \frac{\partial^4 v}{\partial y^2 \partial z^2}(0, y, z, t), \quad t \in [t_s, t_{s+1}). \end{aligned} \quad (13)$$

Now, Integrate equation (13) twice w.r.t  $y$  from 0 to  $y$  also using the boundary conditions, we get

$$\begin{aligned} \frac{\partial^2 v}{\partial z^2}(x, y, z, t) &= (t - t_s) \sum_{i,j,k=1}^{2M} \alpha_{i,j,k} P_{2,i}(x) P_{2,j}(y) h_k(z) + \frac{\partial^2 v}{\partial z^2}(x, y, z, t_s) - \frac{\partial^2 v}{\partial z^2}(x, 0, z, t_s) - \frac{\partial^2 v}{\partial z^2}(0, y, z, t_s) \\ &+ \frac{\partial^2 v}{\partial z^2}(0, 0, z, t_s) + \frac{\partial^2 v}{\partial z^2}(0, y, z, t) - \frac{\partial^2 v}{\partial z^2}(0, 0, z, t) + \frac{\partial^2 v}{\partial z^2}(x, 0, z, t), \quad t \in [t_s, t_{s+1}). \end{aligned} \quad (14)$$

Similarly, Integrate equation (13) twice w.r.t  $z$  from 0 to  $z$  also using the boundary conditions, we get

$$\begin{aligned} \frac{\partial^2 v}{\partial y^2}(x, y, z, t) &= (t - t_s) \sum_{i,j,k=1}^{2M} \alpha_{i,j,k} P_{2,i}(x) h_j(y) P_{2,k}(z) + \frac{\partial^2 v}{\partial y^2}(x, y, z, t_s) - \frac{\partial^2 v}{\partial y^2}(x, y, 0, t_s) - \frac{\partial^2 v}{\partial y^2}(0, y, z, t_s) \\ &+ \frac{\partial^2 v}{\partial y^2}(0, y, 0, t_s) + \frac{\partial^2 v}{\partial y^2}(0, y, z, t) - \frac{\partial^2 v}{\partial y^2}(0, y, 0, t) + \frac{\partial^2 v}{\partial y^2}(x, y, 0, t), \quad t \in [t_s, t_{s+1}). \end{aligned} \quad (15)$$

Again, Integrating (12) twice w.r.t  $z$  from 0 to  $z$  and then twice w.r.t  $y$  from 0 to  $y$  also using the boundary conditions, we get

$$\begin{aligned} \frac{\partial^2 v}{\partial x^2}(x, y, z, t) &= (t - t_s) \sum_{i,j,k=1}^{2M} \alpha_{i,j,k} h_i(x) P_{2,j}(y) P_{2,k}(z) + \frac{\partial^2 v}{\partial x^2}(x, y, z, t_s) - \frac{\partial^2 v}{\partial x^2}(x, 0, z, t_s) - \frac{\partial^2 v}{\partial x^2}(x, y, 0, t_s) \\ &+ \frac{\partial^2 v}{\partial x^2}(x, 0, 0, t_s) + \frac{\partial^2 v}{\partial x^2}(x, 0, z, t) - \frac{\partial^2 v}{\partial x^2}(x, 0, 0, t) + \frac{\partial^2 v}{\partial x^2}(x, y, 0, t), \quad t \in [t_s, t_{s+1}]. \end{aligned} \quad (16)$$

Now, Integrate equation (10) twice w.r.t.  $x$ ,  $y$  and then  $z$  also using boundary conditions, we will obtain

$$\begin{aligned} \frac{\partial v}{\partial t}(x, y, z, t) &= \sum_{i,j,k=1}^{2M} \alpha_{i,j,k} P_{2,i}(x) P_{2,j}(y) P_{2,k}(z) + \frac{\partial v}{\partial t}(0, y, z, t) - \frac{\partial v}{\partial t}(0, y, 0, t) - \frac{\partial v}{\partial t}(0, 0, z, t) + \frac{\partial v}{\partial t}(0, 0, 0, t) \\ &+ \frac{\partial v}{\partial t}(x, 0, z, t) - \frac{\partial v}{\partial t}(x, 0, 0, t) + \frac{\partial v}{\partial t}(x, y, 0, t), \quad t \in [t_s, t_{s+1}]. \end{aligned} \quad (17)$$

Now, Integrating the above equation (17) w.r.t.  $t$  from  $t_s$  to  $t$ , we will get

$$\begin{aligned} v(x, y, z, t) &= (t - t_s) \sum_{i,j,k=1}^{2M} \alpha_{i,j,k} P_{2,i}(x) P_{2,j}(y) P_{2,k}(z) + v(x, y, z, t_s) + v(0, y, z, t) - v(0, y, z, t_s) - v(0, y, 0, t) \\ &+ v(0, y, 0, t_s) - v(0, 0, z, t) + v(0, 0, z, t_s) + v(0, 0, 0, t) - v(0, 0, 0, t_s) + v(x, 0, z, t) - v(x, 0, z, t_s) \\ &- v(x, 0, 0, t) + v(x, 0, 0, t_s) + v(x, y, 0, t) - v(x, y, 0, t_s). \end{aligned} \quad (18)$$

Again, Integrate (11) w.r.t  $t$  from  $t_s$  to  $t$ , we acquire

$$w(x, y, z, t) = (t - t_s) \sum_{l,m,n=1}^{2M} \beta_{l,m,n} h_l(x) h_m(y) h_n(z) + w(x, y, z, t_s) \quad (19)$$

To find the solution at the collocation points, we have to discretized the equation (7) and (8) when  $t \rightarrow t_{s+1}$ .

The discrete form is as follows:

$$\begin{aligned} \epsilon(x_{k_1}, y_{k_2}, z_{k_3}) \frac{\partial v}{\partial t}(x_{k_1}, y_{k_2}, z_{k_3}, t_{s+1}) &- \left[ \sigma_l(x_{k_1}, y_{k_2}, z_{k_3}) \frac{\partial^2 v}{\partial x^2}(x_{k_1}, y_{k_2}, z_{k_3}, t_{s+1}) + \sigma_{l,x}(x_{k_1}, y_{k_2}, z_{k_3}) \frac{\partial v}{\partial x}(x_{k_1}, y_{k_2}, z_{k_3}, t_{s+1}) \right. \\ &+ (\sigma_t(x_{k_1}, y_{k_2}, z_{k_3})) \frac{\partial^2 v}{\partial y^2}(x_{k_1}, y_{k_2}, z_{k_3}, t_{s+1}) + \sigma_{t,y}(x_{k_1}, y_{k_2}, z_{k_3}) \frac{\partial v}{\partial y}(x_{k_1}, y_{k_2}, z_{k_3}, t_{s+1}) + \sigma_t(x_{k_1}, y_{k_2}, z_{k_3}) \\ &\left. \frac{\partial^2 v}{\partial z^2}(x_{k_1}, y_{k_2}, z_{k_3}, t_{s+1}) + \sigma_{t,z}(x_{k_1}, y_{k_2}, z_{k_3}) \frac{\partial v}{\partial z}(x_{k_1}, y_{k_2}, z_{k_3}, t_{s+1}) \right] + f(v(x_{k_1}, y_{k_2}, z_{k_3}, t_{s+1}), w(x_{k_1}, y_{k_2}, z_{k_3}, \\ &t_{s+1})) = 0, \end{aligned} \quad (20)$$

$$\frac{\partial w}{\partial t}(x_{k_1}, y_{k_2}, z_{k_3}, t_{s+1}) = g(v(x_{k_1}, y_{k_2}, z_{k_3}, t_{s+1}), w(x_{k_1}, y_{k_2}, z_{k_3}, t_{s+1})). \quad (21)$$

Using (11) at the grid points in (21) and linearize the non-linear terms by treating it explicitly, we obtain the following

$$\sum_{l,m,n=1}^{2M} \beta_{l,m,n} h_l(x_{k_1}) h_m(y_{k_2}) h_n(z_{k_3}) = g(v(x_{k_1}, y_{k_2}, z_{k_3}, t_s), w(x_{k_1}, y_{k_2}, z_{k_3}, t_s)).$$

Matrix system of the above equation is given by,

$$H_l H_m H_n \beta = c, \quad (22)$$

where  $H_l, H_m, H_n$  are the Haar matrices and  $c^t = (c_{k_1, k_2, k_3})$ , which is given by,

$$c_{k_1, k_2, k_3} = g(v(x_{k_1}, y_{k_2}, z_{k_3}, t_s), w(x_{k_1}, y_{k_2}, z_{k_3}, t_s)). \quad (23)$$

Now, at each time step we will calculate the wavelet coefficient  $\beta$  and then from (19) at the collocation points we will calculate the solution  $w$ . So, now we will use this  $w$  to calculate the solution  $v$ .

Again, Calculate equations (15), (16) and (17) at the collocation points and substitute in (20) and (21) and treat non-linear terms explicitly in  $v$ , we get the following equation in matrix form at time  $t_{s+1}$ :

$$K\alpha = b, \quad (24)$$

where  $K = (k_{ij})$  is a matrix of size  $8M^3 \times 8M^3$  and  $b$  is a column vector of size  $8M^3 \times 1$ .

Now from the above equation we will calculate the wavelet coefficient  $\alpha$  and then obtain the solution  $v$  with the use of calculated  $w$ , at the desired time step.

#### 4 Convergence Analysis

**Lemma 1** *If  $v(x, y, z)$  and  $w(x, y, z)$  are Lipschitz continuous on domain  $[0, 1]^3$ , then the wavelet coefficients  $a_{i_1, i_2, i_3}$ ,  $b_{l_1, l_2, l_3}$  corresponding to  $v$  and  $w$  satisfy the inequality*

$$|a_{i_1, i_2, i_3}| \leq \frac{L}{8m^4}, \quad (25)$$

$$|b_{l_1, l_2, l_3}| \leq \frac{L}{8m^4}, \quad (26)$$

where  $L > 0$  depends on the Lipschitz constant and the coefficients are defined as

$$a_{i_1, i_2, i_3} = \int_0^1 \int_0^1 v(x, y, z) h_{i_1}(x) h_{i_2}(y) h_{i_3}(z) dx dy dz, \quad (27)$$

$$b_{l_1, l_2, l_3} = \int_0^1 \int_0^1 w(x, y, z) h_{l_1}(x) h_{l_2}(y) h_{l_3}(z) dx dy dz, \quad (28)$$

Proof: We can redefine the definition of the coefficient  $a_{i_1, i_2, i_3}$  in terms of the inner product as follows

$$a_{i_1, i_2, i_3} = \int_0^1 \int_0^1 v(x, y, z) h_{i_1}(x) h_{i_2}(y) h_{i_3}(z) dx dy dz = \langle h_{i_1}(x), \langle h_{i_2}(y), \langle v(x, y, z), h_{i_3}(z) \rangle \rangle \rangle,$$

where  $\langle \cdot \rangle$  is defined as the inner product.

$$\langle v(x, y, z), h_{i_3}(z) \rangle = \int_0^1 v(x, y, z) h_{i_3}(z) dz.$$

Using the definition of Haar wavelet, we get

$$\langle v(x, y, z), h_{i_3}(z) \rangle = \int_{\frac{k}{m}}^{\frac{k+0.5}{m}} v(x, y, z) dz - \int_{\frac{k+0.5}{m}}^{\frac{k+1}{m}} v(x, y, z) dz.$$

Now, applying the Mean Value theorem for both the integrals, we find an  $z_1 \in \left(\frac{k}{m}, \frac{k+0.5}{m}\right)$  and an  $z_2 \in \left(\frac{k+0.5}{m}, \frac{k+1}{m}\right)$  such that

$$\begin{aligned} \langle v(x, y, z), h_{i_3}(z) \rangle &= \left(\frac{k+0.5}{m} - \frac{k}{m}\right) v(x, y, z_1) - \left(\frac{k+1}{m} - \frac{k+0.5}{m}\right) v(x, y, z_2) \\ &= \frac{1}{2m} [v(x, y, z_1) - v(x, y, z_2)]. \end{aligned}$$

Now,

$$\langle h_{i_2}(y), \langle v(x, y, z), h_{i_3}(z) \rangle \rangle = \frac{1}{2m} \left\{ \int_0^1 v(x, y, z_1) h_j(y) dy - \int_0^1 v(x, y, z_2) h_j(y) dy \right\}.$$

Again, using the definition of Haar wavelet in both the integral, we obtain



$$\begin{aligned} \langle h_{i_2}(y), \langle v(x, y, z), h_{i_3}(z) \rangle \rangle &= \frac{1}{2m} \left[ \left\{ \int_{\frac{k}{m}}^{\frac{k+0.5}{m}} v(x, y, z_1) dy - \int_{\frac{k+0.5}{m}}^{\frac{k+1}{m}} v(x, y, z_1) dy \right\} \right. \\ &\quad \left. - \left\{ \int_{\frac{k}{m}}^{\frac{k+0.5}{m}} v(x, y, z_2) dy - \int_{\frac{k+0.5}{m}}^{\frac{k+1}{m}} v(x, y, z_2) dy \right\} \right]. \end{aligned}$$

Now, applying the Mean Value Theorem for all the four integrals, we find  $y_1, y_2 \in \left(\frac{k}{m}, \frac{k+0.5}{m}\right)$  and  $y_3, y_4 \in \left(\frac{k+0.5}{m}, \frac{k+1}{m}\right)$  such that

$$\langle h_{i_2}(y), \langle v(x, y, z), h_{i_3}(z) \rangle \rangle = \frac{1}{4m^2} \left[ v(x, y_1, z_1) - v(x, y_2, z_1) - v(x, y_3, z_2) + v(x, y_4, z_2) \right].$$

Hence,

$$\begin{aligned} a_{i_1, i_2, i_3} &= \langle h_{i_1}(x), \langle h_{i_2}(y), \langle v(x, y, z), h_{i_3}(z) \rangle \rangle \rangle \\ &= \frac{1}{4m^2} \left\{ \int_0^1 v(x, y_1, z_1) h_{i_1}(x) dx - \int_0^1 v(x, y_2, z_1) h_{i_1}(x) dx - \int_0^1 v(x, y_3, z_2) h_{i_2}(x) dx + \int_0^1 v(x, y_4, z_2) h_{i_2}(x) dx \right\} \end{aligned}$$

Using the definition of Haar wavelet in all the integral and then the Mean Value Theorem, we have we find  $x_1, x_2, x_3, x_4 \in \left(\frac{k}{m}, \frac{k+0.5}{m}\right)$  and  $x_5, x_6, x_7, x_8 \in \left(\frac{k+0.5}{m}, \frac{k+1}{m}\right)$  such that

$$\begin{aligned} |a_{i_1, i_2, i_3}| &\leq \frac{1}{8m^3} \left[ |v(x_1, y_1, z_1) - v(x_2, y_1, z_1)| + |v(x_3, y_2, z_1) - v(x_4, y_2, z_1)| \right. \\ &\quad \left. + |v(x_5, y_3, z_2) - v(x_6, y_3, z_2)| + |v(x_7, y_4, z_2) - v(x_8, y_4, z_2)| \right]. \end{aligned}$$

Now, using the Lipschitz continuity of  $v$ , we get

$$|a_{i_1, i_2, i_3}| \leq \frac{1}{8m^3} \{L_1|x_1 - x_2| + L_2|x_3 - x_4| + L_3|x_5 - x_6| + L_4|x_7 - x_8|\},$$

where,  $L_1, L_2, L_3, L_4$  are the Lipschitz constants.

Choose  $L = \max(L_1, L_2, L_3, L_4)$  and from the definition of Haar wavelet we can conclude that  $|x_i - x_j| \leq \frac{1}{2m}$ , we obtain

$$\begin{aligned} |a_{i_1, i_2, i_3}| &\leq \frac{1}{8m^3} \left( \frac{4L}{2m} \right) \\ &= \frac{L}{8m^4}. \end{aligned}$$

Similarly, the wavelet coefficient  $b_{l_1, l_2, l_3}$  can also be determined.

- Now, introducing the norm as follows:

$$\|u\|_X = \|v\|_2 + \sum_{k=1}^d \|w^k\|_2, \quad (29)$$

where  $\|\cdot\|_2$  is the  $L^2([0, 1]^3)$ -norm.

Let  $u = [v \ w]$  be the exact solution of the problem and  $u_H = [v_H \ w_H]$  be the solution approximated by the Haar wavelets. The error ( $E = u - u_H$ ) is given as follows:

**Theorem 1** Let  $u$  be the exact solution of the problem and  $u_H$  be the solution approximated by the Haar wavelets, then

$$\| E \|_X^2 = \| u(x, y, t_{n+1}) - u_H(x, y, t_{n+1}) \|_X^2 \leq C dt^2 \left[ \frac{K_1 K_2 K_3}{m^2} + \frac{d}{m^8} \right], \quad (30)$$

which implies that  $\| E \|_X^2 \rightarrow 0$  as  $dt \rightarrow 0$  and  $m \rightarrow \infty$ .

Proof. Calculate the error using equations (18) and (19) for the Haar wavelet solution, we obtain the following

$$\begin{aligned} \| E \|_X^2 &= \| dt \sum_{i_1, i_2, i_3=2M+1}^{\infty} a_{i_1, i_2, i_3} P_{2, i_1}(x) P_{2, i_2}(y) P_{2, i_3}(z) \|_2^2 + \sum_{w=1}^d \| dt \sum_{l_1, l_2, l_3=2M+1}^{\infty} b_{l_1, l_2, l_3}^w H_{l_1}(x) H_{l_2}(y) H_{l_3}(z) \|_2^2 \\ &= dt^2 \int_0^1 \int_0^1 \left| \sum_{i_1, i_2, i_3=2M+1}^{\infty} a_{i_1, i_2, i_3} P_{2, i_1}(x) P_{2, i_2}(y) P_{2, i_3}(z) \sum_{p, q, r=2M+1}^{\infty} a_{p, q, r} P_{2, p}(x) P_{2, q}(y) P_{2, r}(z) \right| \\ &\quad + \sum_{w=1}^d \| dt^2 \int_0^1 \int_0^1 \left| \sum_{l_1, l_2, l_3=2M+1}^{\infty} b_{l_1, l_2, l_3}^w H_{l_1}(x) H_{l_2}(y) H_{l_3}(z) \sum_{s, t, h=2M+1}^{\infty} b_{s, t, h}^k H_s(x) H_t(y) H_h(z) \right|, \\ &\leq dt^2 \sum_{i_1, i_2, i_3=2M+1}^{\infty} |a_{i_1, i_2, i_3}| \sum_{p, q, r=2M+1}^{\infty} |a_{p, q, r}| \left( \int_0^1 |P_{2, i_1}(x) P_{2, p}(x)| dx \right) \left( \int_0^1 |P_{2, i_2}(y) P_{2, q}(y)| dy \right) \\ &\quad \left( \int_0^1 |P_{2, i_3}(z) P_{2, r}(z)| dz \right) + dt^2 \sum_{w=1}^d \left[ \sum_{l_1, l_2, l_3=2M+1}^{\infty} |b_{l_1, l_2, l_3}^w| \sum_{s, t, h=2M+1}^{\infty} |b_{s, t, h}^k| \left( \int_0^1 |H_{l_1}(x) H_s(x)| dx \right) \right. \\ &\quad \left. \left( \int_0^1 |H_{l_2}(y) H_t(y)| dy \right) \left( \int_0^1 |H_{l_3}(z) H_h(z)| dz \right) \right] \\ &= dt^2 \sum_{i_1, i_2, i_3=2M+1}^{\infty} |a_{i_1, i_2, i_3}| \sum_{p, q, r=2M+1}^{\infty} |a_{p, q, r}| K_{i_1, p} K_{i_2, q} K_{i_3, r} + dt^2 \sum_{w=1}^d \left[ \sum_{l_1, l_2, l_3=2M+1}^{\infty} |b_{l_1, l_2, l_3}^w| \sum_{p, q, r=2M+1}^{\infty} |b_{p, q, r}^k| L_{l_1, s} \right. \\ &\quad \left. L_{l_2, t} L_{l_3, h} \right], \\ &= I_1 + I_2, \end{aligned}$$

where,

$$\begin{aligned} K_{i_1, p} &= \int_0^1 |P_{2, i_1}(x) P_{2, p}(x)| dx, \\ K_{i_2, q} &= \int_0^1 |P_{2, i_2}(y) P_{2, q}(y)| dy, \\ K_{i_3, r} &= \int_0^1 |P_{2, i_3}(z) P_{2, r}(z)| dz, \end{aligned}$$

and

$$\begin{aligned} L_{l_1, s} &= \int_0^1 |H_{l_1}(x) H_s(x)| dx, \\ L_{l_2, t} &= \int_0^1 |H_{l_2}(y) H_t(y)| dy, \\ L_{l_3, h} &= \int_0^1 |H_{l_3}(z) H_h(z)| dz. \end{aligned}$$

Let  $K_{i_1} = \sup_r K_{i_1, p}$ ,  $K_{i_2} = \sup_s K_{i_2, q}$ , and,  $K_{i_3} = \sup_s K_{i_3, r}$  first term ( $I_1$ ) becomes as

$$\begin{aligned}
I_1 &\leq dt^2 \sum_{i_1, i_2, i_3=2M+1}^{\infty} |a_{i_1, i_2, i_3}| K_{i_1} K_{i_2} K_{i_3} \sum_{p, q, r=2M+1}^{\infty} |a_{p, q, r}| \\
&\leq \frac{Ldt^2}{8} \sum_{i_1, i_2, i_3=2M+1}^{\infty} |a_{i_1, i_2, i_3}| K_{i_1} K_{i_2} K_{i_3} \sum_{j=J+1}^{\infty} \sum_{p, q, r}^{2^j-1} \frac{1}{m^4}, \text{ using Lemma 3} \\
&\leq \frac{Ldt^2}{8} \sum_{i_1, i_2, i_3=2M+1}^{\infty} |a_{i_1, i_2, i_3}| K_{i_1} K_{i_2} K_{i_3} \frac{1}{m}
\end{aligned}$$

Now, let  $K_1 = \sup_{i_1} K_{i_1}$ ,  $K_2 = \sup_{i_2} K_{i_2}$ , and,  $K_3 = \sup_{i_3} K_{i_3}$  we obtain

$$\begin{aligned}
I_1 &\leq \frac{Ldt^2}{8} K_1 K_2 K_3 \sum_{i_1, i_2, i_3=2M+1}^{\infty} |a_{i_1, i_2, i_3}| \frac{1}{m} \\
&\leq \frac{L^2 dt^2}{64} K_1 K_2 K_3 \sum_{j=J+1}^{\infty} \sum_{i_1, i_2, i_3=0}^{2^j-1} \frac{1}{m^5}, \text{ using Lemma 3} \\
&\leq \frac{L^2 dt^2 K_1 K_2 K_3}{64m^2}
\end{aligned}$$

Again, we know by the definition of Haar wavelet ,

$$\int_0^1 H_{l_1}(x) H_p(x) dx = 2^{-j} = \frac{1}{m}$$

$$\begin{aligned}
I_2 &= (dt)^2 \sum_{w=1}^d \left[ \sum_{l_1, l_2, l_3=2M+1}^{\infty} |b_{l_1, l_2, l_3}^{q1}|^2 \frac{1}{m^3} \right] \\
&\leq \frac{L^2 dt^2}{64} \sum_{w=1}^d \left( \frac{1}{m^4} \right)^2, \text{ using Lemma 3} \\
&\leq \frac{dL^2 dt^2}{16m^8}
\end{aligned}$$

Therefore,

$$\begin{aligned}
\| E \|_X^2 &\leq \frac{C^2 dt^2 K_1 K_2 K_3}{64m^2} + \frac{dC^2 dt^2}{64m^8} \\
&\leq C dt^2 \left[ \frac{K_1 K_2 K_3}{m^2} + \frac{d}{m^8} \right]
\end{aligned}$$

*Algorithm to calculate the Haar wavelet solution*

- Step1: Calculate the Haar matrix  $H$  and the Haar Integral matrix  $P_1$  and  $P_2$  by using the equations (1) and (3) respectively.
- Step2: Compute  $c$  using the equation (23) and then solve the matrix equation  $H\alpha = c$  to find the wavelet coefficient  $\beta$ .
- Step3: Use the wavelet coefficient  $\beta$  in equation (19) and the given initial values of  $v$  and  $w$  at the to compute the gating variable  $w$ .
- Step4: Compute the matrix  $K$  and the vector  $b$ . Use the above calculated gating variables  $w$  and solve the matrix equation  $K\alpha = b$  to find the wavelet coefficient  $\alpha$  and then use  $\alpha$  in (18) to compute the solution  $v$ .

**Remark:** (1) Theorem 1 implies the stability of the solution and theorem 2 implies that the truncation error goes to zero and hence in conjunction they implies the convergence of the solution.

(2) If there is discontinuity in the parameter of the function  $f(v, w)$ ,  $g(v, w)$  or the coefficient  $\epsilon$ ,  $D(x, y)$  , it can be handled using Haar wavelet interpolation.

## 5 Numerical Result and Discussions

To demonstrate the power of Haar wavelet method we presented a few examples which are related to the pathological case studies in cardiac electrical activity. We solve all the examples using the above developed Haar wavelet method and calculate the absolute error also. Grid validation test or resolution level test has been done for all the problems and here we are presenting for some of the problems. From grid validation we observe that resolution level  $J = 4$  in two dimension is good enough to calculate the solution. We also compare the Haar wavelet solution with the solution obtained using the finite element method for almost all the problems. We also calculate the CPU time for Haar wavelet method and the finite element method. For all the examples, we use the GMRES solver to solve the linear system of equations obtained from the discrete problem as it is more appropriate in terms of the CPU time in comparison to the other solvers like, CGS, BICG and BICGSTAB in terms of the CPU time (see Table (5)).

**Example 1.** We consider the one dimensional reaction-diffusion system coupled with the ODE having homogeneous Neumann boundary. Such type of coupled systems are important because it models the problems related to the field of cardiac electrical activity of any species. We will also discuss the problem with jump discontinuity in the parameter or coefficients which is related to the problem of ischemia in cardiac tissue.

$$\begin{aligned} \epsilon \frac{\partial v}{\partial t} - d \frac{d}{dx} \left( \frac{dv}{dx} \right) + kv(v - 0.1)(1 - v) - kw &= I_{app}, & 0 \leq x \leq 1, 0 \leq t \leq T \\ \frac{\partial w}{\partial t} &= v - 2w, & 0 \leq x \leq 1, 0 \leq t \leq T \\ v(x, 0) = 0.2, \quad w(x, 0) &= 0.2, & 0 \leq x \leq 1 \\ \frac{dv}{dx}(0, t) = 0, \quad \frac{dv}{dx}(1, t) &= 0 = 0, & 0 \leq t \leq T \end{aligned}$$

where,  $d = 0.005$  and  $\epsilon = 0.01$ .

Resolution level test for the proposed Haar wavelet method has been presented in Fig. 3.

Pointwise absolute error for different time steps is shown in Table 1. Solution at  $dt = 10^{-5}$ ,  $J = 8$  is taken as the reference solution. From the Table 1, it can be seen clearly that absolute error decreases significantly with the smaller time step size. The Haar wavelet solution for  $v$  at the grid points is presented in Fig. 4. We also solved the same problem using the linear finite element in space and implicit-explicit (IE) Euler method in time. It is observed that the Haar wavelet solution matches with the finite element solution (Fig. 5).

x	absolute error	
	$dt = 10^{-3}$	$dt = 10^{-4}$
0.1406	$6.4 \times 10^{-3}$	$6.2 \times 10^{-4}$
0.2656	$6.9 \times 10^{-3}$	$6.085 \times 10^{-4}$
0.3594	$8.1 \times 10^{-3}$	$5.464 \times 10^{-4}$
0.4531	$8.8 \times 10^{-3}$	$5.4 \times 10^{-4}$

Table 1: (For example 1) Absolute Error for  $v$  at different points of the domain when  $J = 8$  and  $T=1$ .

From Fig. 5 we can see that when  $I_{app} = 0$ , variable  $v$  goes to the resting state without shooting up. But as we provide  $I_{app} = 0.3$ , the solution  $v$  shoot up from the initial state and then it goes down slowly to the stabilizing state. This type of problems models pathological phenomena like FitzHugh Nagumo (FHN) model in cardiac electrical activity, which is the reduced ionic model of animal.

Next, we consider the same problem but with a jump discontinuity in the parameter  $k$ , drawn in Fig. 6a which creates the local ischemia in a cardiac tissue. We calculate the solution  $v$  at the points, as a sample, in Fig (6b) we present the solution corresponding to the points  $x = 0.2656$  and  $x = 0.4531$ , which lie outside and inside the jump region respectively. The absence of any spurious oscillation in the solution presented in Fig. 6b indicated that Haar wavelets efficiently handle this jump discontinuity.

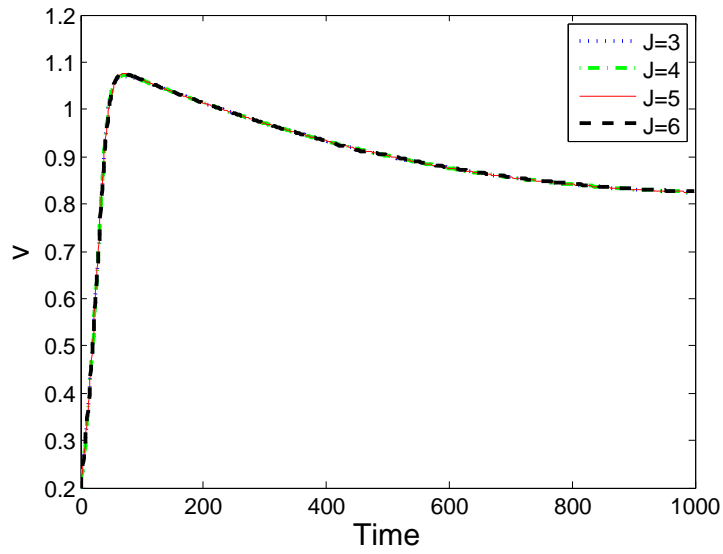


Fig. 3: Resolution level test for Haar wavelet solution  $v$

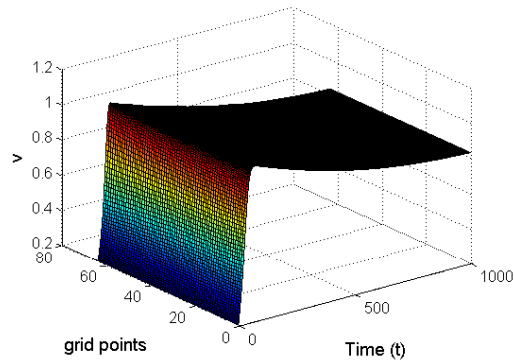


Fig. 4: (for example1) Haar wavelet solution for  $v$ .  $I_{app} = 0.3$ .

*Example 2* We will consider the two dimensional problems which are important in the field of cardiac electrophysiology. We will calculate the transmembrane potential in the heart which is important to know the functionality of the heart. We will solve the problem having jump discontinuity in any parameter or coefficients

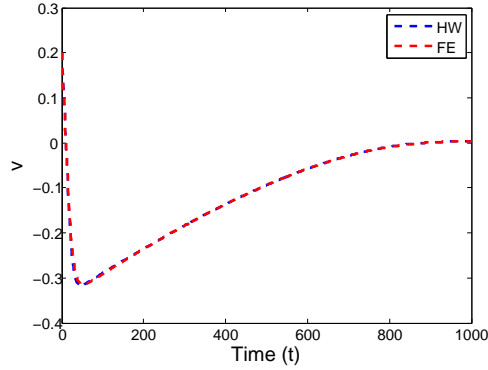


Fig. 5: FE and HW solution at  $x=0.5$ .  $I_{app} = 0$ ,  $J=5$ ,  $dt = 10^{-3}$  and  $T=1$ .

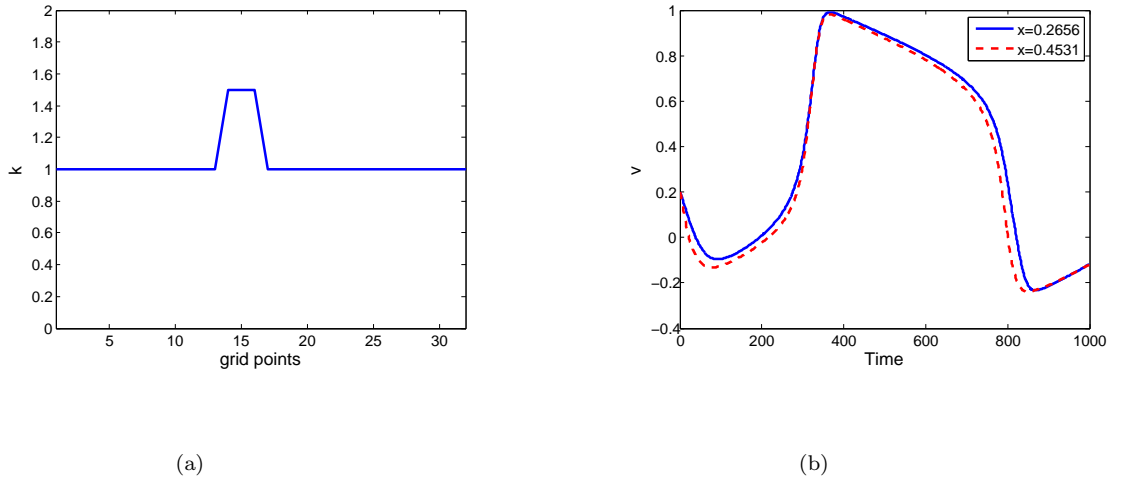


Fig. 6: (a) parameter  $k$ , (b) Corresponding Haar wavelet solution  $v$  at the points falling inside and outside the jump region.  $I_{app} = 0.15$

using the Haar wavelets.

$$\begin{aligned}
 \epsilon \frac{\partial v}{\partial t} - \text{div}(D\nabla v) + kv(v - 0.1)(1 - v) - kw &= I_{app}, & 0 \leq x, y \leq 1, 0 \leq t \leq T \\
 \frac{\partial w}{\partial t} &= v - 2w, & 0 \leq x, y \leq 1, 0 \leq t \leq T \\
 v(x, 0) = 0.2, \quad w(x, 0) &= 0.2, & 0 \leq x, y \leq 1 \\
 \frac{dv}{dx}(0, y, t) &= 0, & 0 \leq t \leq T \\
 \frac{dv}{dx}(1, y, t) &= 0, & 0 \leq t \leq T \\
 \frac{dv}{dy}(x, 0, t) &= 0, & 0 \leq t \leq T \\
 \frac{dv}{dy}(x, 1, t) &= 0, & 0 \leq t \leq T
 \end{aligned}$$

where  $D = \begin{bmatrix} 1.2e-3 & 0 \\ 0 & 2.5562e-4 \end{bmatrix}$ ,  $\epsilon = 0.01$  and  $I_{app} = 0.15$ .

First of all the grid validation of the proposed algorithm for this problem is presented in Fig. 7 which clearly shows the accuracy of the solution at the different resolution level. So, resolution level  $J = 4$  is good enough to calculate the results.

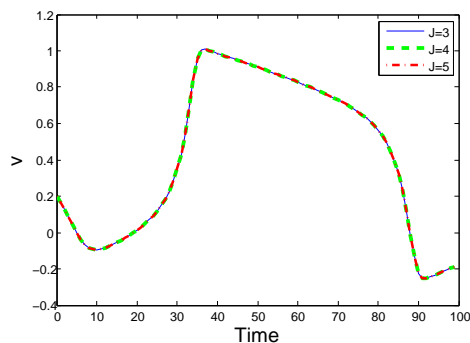


Fig. 7: **Resolution level test for Haar wavelet solution  $v$**

Absolute error for different time steps is shown in Table 2. Solution at  $dt = 10^{-5}$ ,  $J = 6$  is taken as the reference solution. From the Table 2 it can be seen clearly that absolute error decreases seriously with the smaller time step size.

Pointwise absolute error of the Haar wavelet solution  $v$  is presented in Fig.8a. Haar wavelet solution in surface is shown in Fig. 9a and Fig. 9b respectively. We also solved the same problem using the linear finite element in space and implicit-explicit (IE) Euler method in time. Haar wavelet solution matches with the finite element solution as shown in Fig. 8b.

Maximum absolute error		
$dt = 10^{-2}$	$dt = 10^{-3}$	$dt = 10^{-4}$
$1.7 \times 10^{-2}$	$1.9 \times 10^{-3}$	$8.3 \times 10^{-5}$

Table 2: Maximum Absolute Error (for example 2) of  $v$  when  $J = 6$  and  $T=0.5$ ,  $k=1$ .

Now, if the parameter  $k$  in the above equation have jump discontinuity at some places in the domain, as shown in Fig. 10a. This jump parameter models the local ischemia in the heart tissue. It is important to calculate the transmembrane potential with this ischemia to know the change in electrical activity of the heart.

The solution  $v$  corresponding to this value of the parameter  $k$  at the points (0.1563,0.1563) (lies outside the jump region) and (0.4688,0.4688) (lies within the jump region of the domain) are drawn in Fig. 10b. There is no oscillation in the solution with discontinuity is noticed also the behavior of the solution clearly depict that Haar wavelets handle the jump discontinuity in the parameter  $k$ .

Again, if the discontinuity is in the parameter  $\epsilon$  of the model equation, like drawn in Fig. 11a. The solution  $v$  corresponding to this value of the parameter  $\epsilon$  at the points (0.1563,0.1563) and (0.4688,0.4688) lies outside and inside the jump region respectively in the domain are presented in Fig. 11b. Behavior of the solution with discontinuity in this parameter conclude that the  $\epsilon$  discontinuity is automatically handled by the Haar wavelets.

*Example 3* We will consider the example which is important in the field of cardiac electrophysiology. This model includes only inward and outward current. It contains four time constants, for the four phases of cardiac action

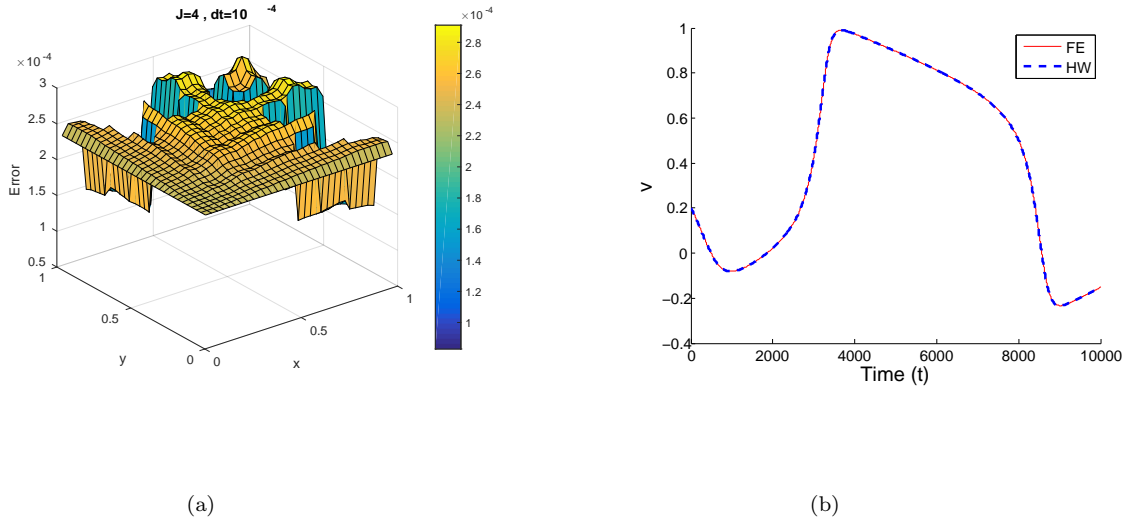


Fig. 8: (a) Numerical error at  $J=6$  and  $T=0.5$  and  $dt = 10^{-4}$ , (b) FE and HW solution comparison at  $J=5$  and  $T=1$  and  $dt = 10^{-4}$ ,  $k = 1$ .

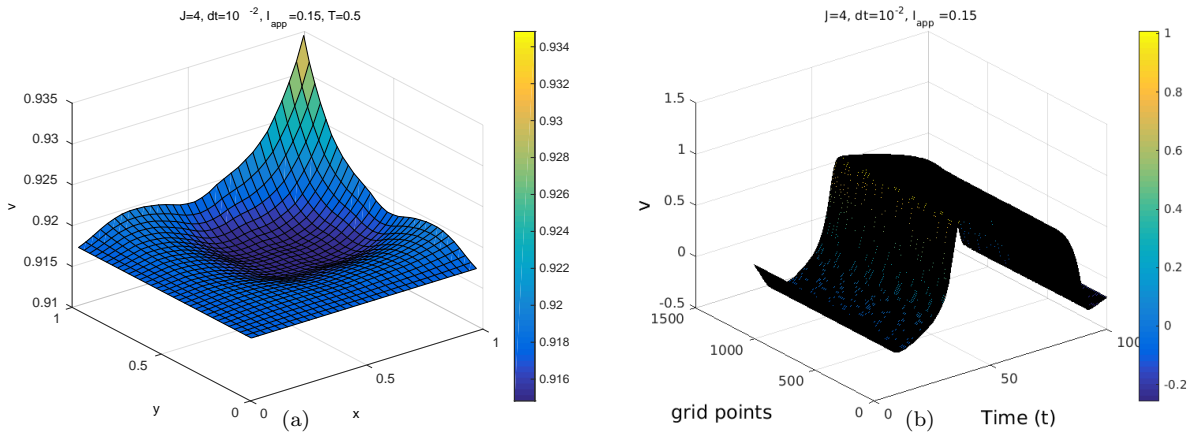


Fig. 9: (a) Surface plot, Haar wavelet solution in 2D, (b) Haar wavelet solution in 2D

potential: initial, plateau, decay and recovery. We will solve the problem having multiple jump discontinuity in any of these parameter using the Haar wavelets.

$$\begin{aligned}
 \frac{\partial v}{\partial t} - \text{div}(D\nabla v) + f(v, w) &= I_{app}, & 0 \leq x, y \leq 1, 0 \leq t \leq T \\
 \frac{\partial w}{\partial t} &= G(v, w), & 0 \leq x, y \leq 1, 0 \leq t \leq T \\
 v(x, 0) = 0.2, \quad w(x, 0) &= 0.2, & 0 \leq x, y \leq 1 \\
 \frac{dv}{dx}(0, y, t) &= 0, & 0 \leq t \leq T \\
 \frac{dv}{dx}(1, y, t) &= 0, & 0 \leq t \leq T \\
 \frac{dv}{dy}(x, 0, t) &= 0, & 0 \leq t \leq T \\
 \frac{dv}{dy}(x, 1, t) &= 0, & 0 \leq t \leq T
 \end{aligned}$$



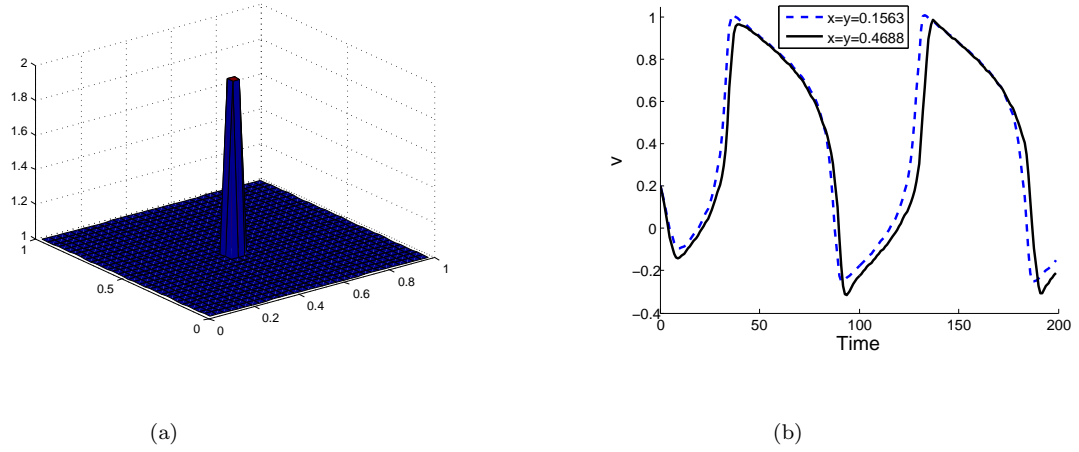


Fig. 10: (a)  $k$  parameter value, (b) Solution for  $v$  with jump discontinuity in  $k$  parameter.

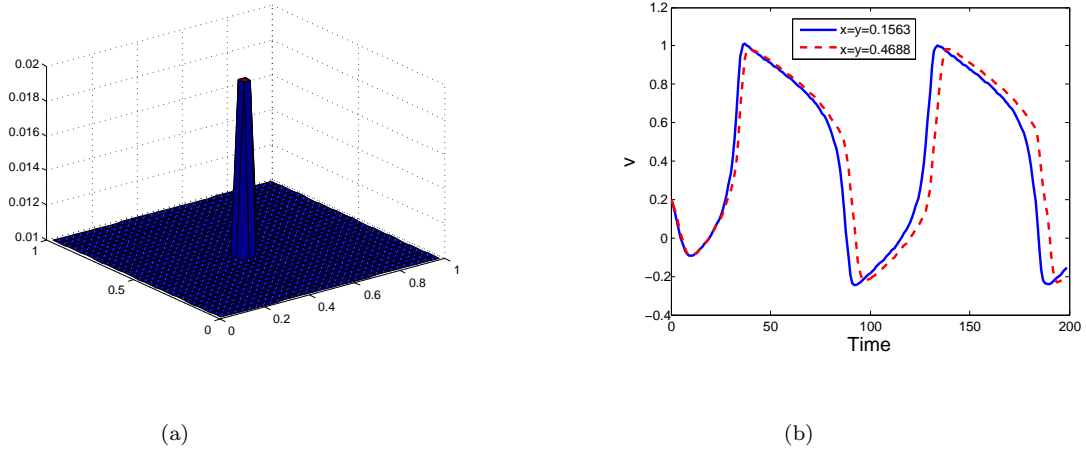


Fig. 11: (a)  $\epsilon$  parameter value, (b) Corresponding solution  $v$ .

where,

$$f(v, w) = -\frac{w}{\tau_{in}} v^2 (v - 1) - \frac{v}{\tau_{out}},$$

$$G(u, w) = \begin{cases} \frac{1-w}{\tau_{open}} & v \leq u_{gate}, \\ \frac{-w}{\tau_{close}} & v > u_{gate}. \end{cases}$$

$$D = \begin{bmatrix} 1.2e-3 & 0 \\ 0 & 2.5562e-4 \end{bmatrix}, \text{ and } I_{app} = \begin{cases} 20 & Nt \leq 100, \\ 0 & o.w. \end{cases}.$$

The solution of this model with the above proposed HW matches with the FE solution, shown in Fig. 12.

Now, if the parameter  $\tau_{in}$  in the above equation have jump discontinuity at some places in the domain, as shown in Fig. 13a and Fig. 15a, the corresponding function  $I_{ion}(v, w)$  will also be discontinuous, shown in Fig. 13b and 15b. This discontinuity is automatically handled using Haar wavelets. The solution  $v$  corresponding to  $\tau_{in}$  in Fig. 13a at the points (0.2344, 0.2344) and (0.4531, 0.4531), lie outside and inside the jump region of the domain are shown in Fig. 14. Now, the solution  $v$  corresponding to  $\tau_{in}$  in Fig. 15a at the points (0.2656, 0.2656), (0.5156, 0.5156) and (0.7344, 0.7344) are presented in Fig. 16. From these Figures, we can clearly see

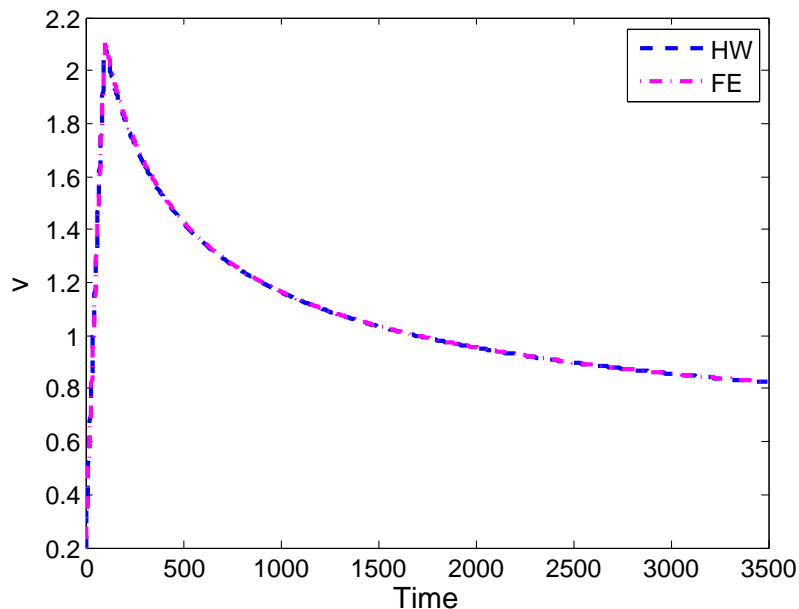


Fig. 12: FE and HW solution comparison at  $J=4$  and  $T=3.5$  and  $dt = 10^{-3}$ .

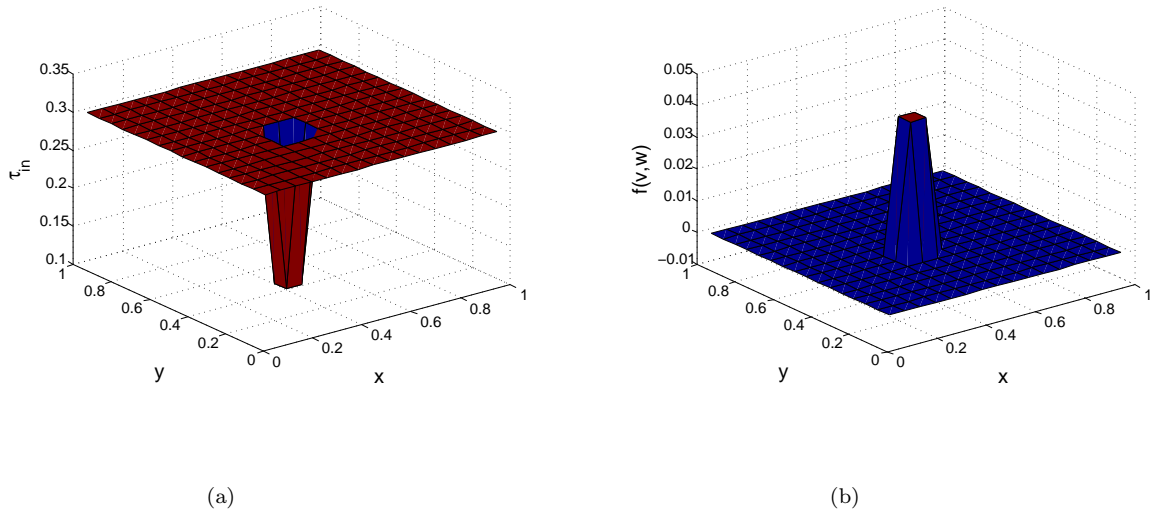
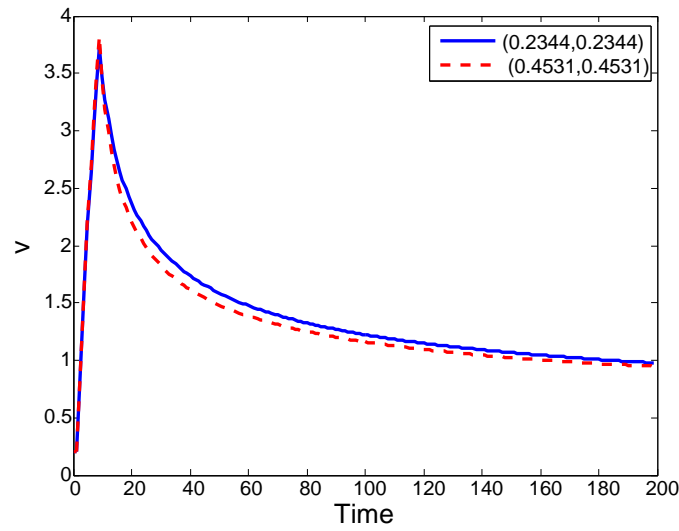
	J	dt	FEM CPU time (sec)	HW CPU time (sec)
Example 2	3 (256 grid)	$10^{-2}$	2.06464	1.690459
	4 (1024 grid)	$10^{-2}$	7.30766	6.40874
Example 3	3 (256 grid)	$10^{-2}$	2.94036	1.527416
	4 (1024 grid)	$10^{-2}$	9.84829	5.342718

Table 3: CPU time 2D

that Haar wavelets automatically handle the multiple jumps in the parameter  $\tau_{in}$ . This clearly describes the power of using Haar wavelets.

This type of single or multiple jump discontinuity problems are useful to calculate the effect of ischemia in the cardiac electrical activity in a tissue with single or multiple ischemic subregions. In such type of problems local ischemia is handled by changing the value of the corresponding parameters into the model at these ischemic subregions only. Thus, Haar wavelet method is a computationally effective tool to solve such types of pathological problems.

Comparison of the computation time of finite element solution and the Haar wavelet solution for 2D model in example 2 and example 3 is presented in Table 3. Clearly, from the table, the haar wavelet method reduces the computational cost in comparison of FEM.

Fig. 13: (a)  $\tau_{in}$  parameter value, (b) Function  $f(v, w)$ .Fig. 14: Solution  $v$  with jump discontinuity in  $\tau_{in}$  parameter.

*Example 4* We will solve the following Monodomain cardiac tissue level model with the complex non-linear Hodgkin-Huxely ionic model Hodgkin and Huxley (1952) using the above developed Haar wavelet method.

$$\begin{aligned}
 \frac{\partial v}{\partial t} - \operatorname{div}(D(x)\nabla v) + I_{ion}(v, w) &= I_{app}, & x \in \Omega, 0 \leq t \leq T \\
 \frac{\partial w}{\partial t} - g(v, w) &= 0, & x \in \Omega, 0 \leq t \leq T \\
 v(x, 0) = v_0(x, 0), \quad w(x, 0) &= w_{i,0}(x, 0), & x \in \Omega \\
 n^T D(x)\nabla v &= 0, & x \in \partial\Omega, 0 \leq t \leq T
 \end{aligned}$$

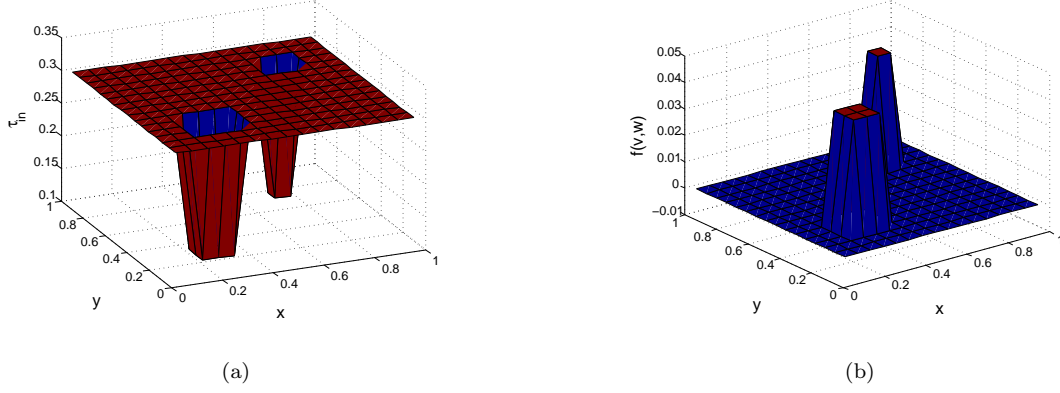


Fig. 15: (a)  $\tau_{in}$  parameter value with jump discontinuity at two regions, (b) Corresponding function  $f(v, w)$ .

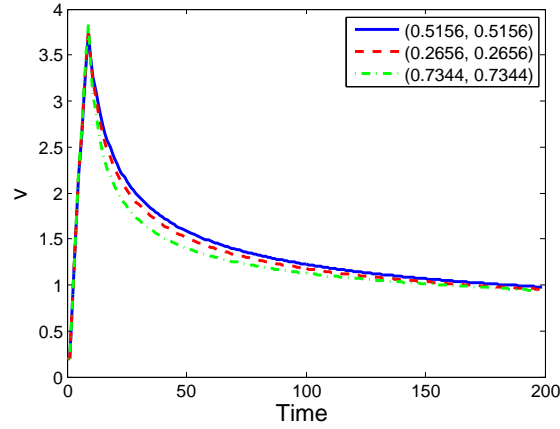


Fig. 16: Solution  $v$  with jump discontinuity at two places in  $\tau_{in}$  parameter.

where,  $I_{app}$  is the applied stimulus and  $D(x)$  is the conductivity tensor defined as:

$$D(x) = \sigma_t I + (\sigma_l - \sigma_t) b_l(x) b_l^t(x) \quad \text{with} \quad \sigma_s = \frac{\tilde{l}\sigma_s^i}{1 + \tilde{l}}, \quad s = l, t, n.$$

$g(v, w)$  and  $I_{ion}(v, w)$  are given by the models at the cell level, called ionic models. Here, we are choosing the Hodgkin Huxely ionic model.

Hodgkin and Huxely in 1952 modeled an ionic model to calculate the action potential in a squid giant axon. In this model, sodium and potassium ionic channels and hence corresponding two separate ionic currents are taken into account. All other small ionic currents are lumped into the leakage current. The model equation is given as follows

$$I_{ion} = g_{Na} m^3 h (v - E_{Na}) + g_K n^4 (v - E_K) + g_L (v - E_L), \quad (31)$$

where,  $g_{Na}$  and  $g_K$  are the maximal conductances corresponding to their membrane which depends on the voltage and time,  $E_{Na}, E_K, E_L$  are the corresponding ion resting potentials.  $I_{app}$  is the externally applied

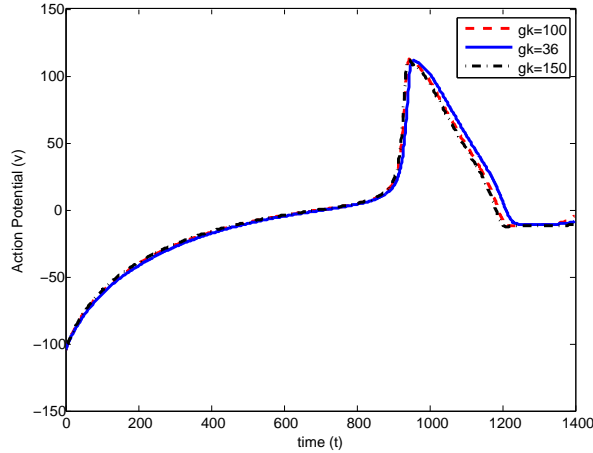


Fig. 17: Action Potential for HH model

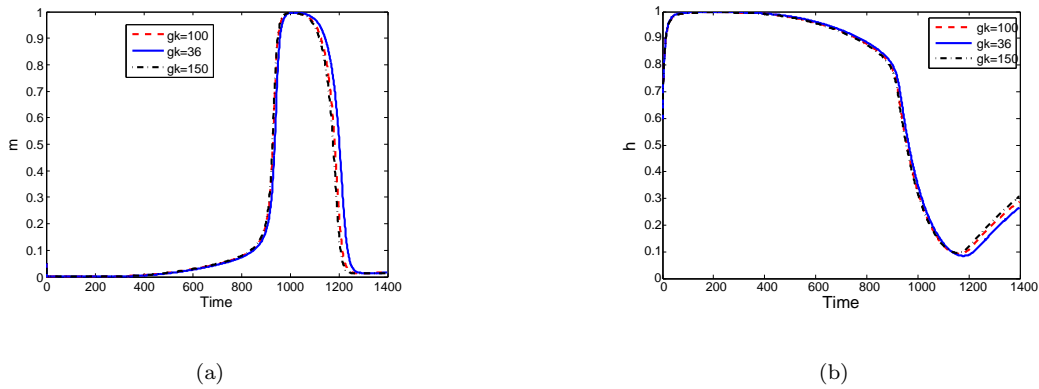


Fig. 18: (a) m gate, (b) h gate.

current.  $m$ ,  $h$  and  $n$  are the gating variables and the dynamics of each of the gating variables is described by the ordinary differential equation:

$$\frac{dw}{dt} = \alpha_w(1 - w) - \beta_w, \quad w = m, h, n, \quad (32)$$

where,  $\alpha_w$  and  $\beta_w$  are the rates depends upon the membrane voltage.

Here, the conductivity of potassium ion  $g_K$  depends on the voltage and time. If we change this parameter value membrane potential or the action potential will also change in the tissue. Action potential and the gating variables for the different value of the parameter is presented in Fig. 17, 18a and 18b.

The jump discontinuity in the parameter  $g_K$  and hence in  $I_{ion}$  is handled by the Haar wavelets.

Now, we are choosing the parameter  $g_k$  value having jump discontinuity at the two subdomains of the domain, as shown in Fig. 19. The corresponding function  $I_{ion}(v, w)$  will also be discontinuous in the corresponding subdomains. The solution  $v$  corresponding to this  $g_k$  at the points  $(0.2156, 0.2156)$ ,  $(0.5156, 0.5156)$  and  $(0.7344, 0.7344)$  is presented in Fig. 20.

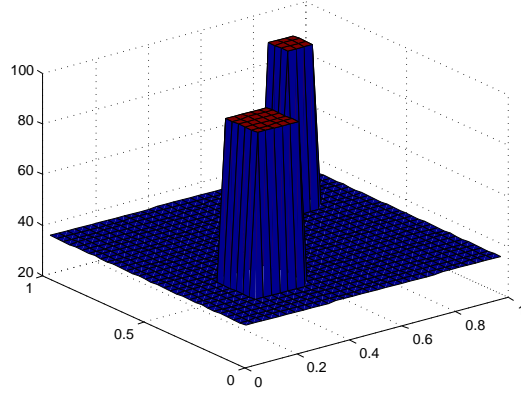


Fig. 19:  $g_K$  parameter value having jump discontinuity at two places,

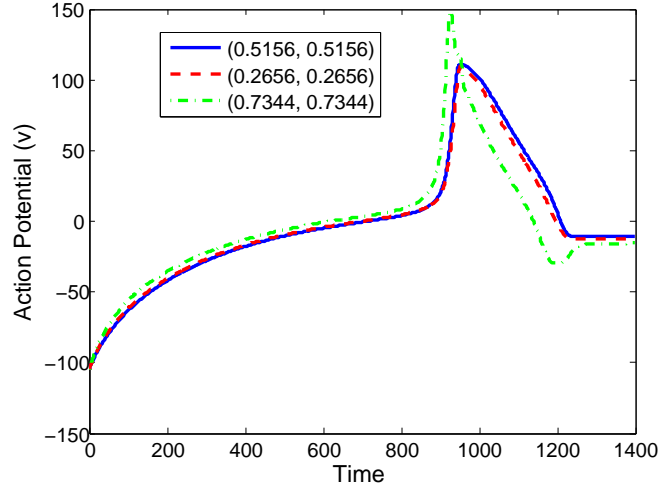


Fig. 20: Action Potential for HH model  $g_K$  parameter value having jump discontinuity at two places.

*Example 5* We will consider the three dimensional example which is important in the field of cardiac electrophysiology. This model includes only inward and outward current. It contains four time constants, for the four phases of cardiac action potential: initial, plateau, decay and recovery. We will solve the problem having jump discontinuity in any of these parameter using the Haar wavelets.

$$\begin{aligned} \frac{\partial v}{\partial t} - \left( d_{11} \frac{\partial^2 v}{\partial x^2} + d_{22} \frac{\partial^2 v}{\partial y^2} + d_{33} \frac{\partial^2 v}{\partial z^2} \right) + I_{ion} &= I_{app}, & 0 \leq x, y, z \leq 1, 0 \leq t \leq T \\ \frac{\partial w}{\partial t} &= v - 2w, & 0 \leq x, y, z \leq 1, 0 \leq t \leq T \\ v(x, y, z, 0) &= 0.2, \quad w(x, y, z, 0) = 0.2, & 0 \leq x, y, z \leq 1 \end{aligned}$$

with Neumann boundary conditions in  $v$ . where,

$$I^{ion} = -\frac{w}{\tau_{in}}u^2(u-1) - \frac{u}{\tau_{out}}$$

$$G(u, w) = \begin{cases} \frac{1-w}{\tau_{open}} & u \leq u_{gate}, \\ \frac{-w}{\tau_{close}} & u > u_{gate}. \end{cases}$$

Comparison of the solution of this system using Haar wavelet method and FEM is presented in Fig. 21. We have drawn the solution along the three cross section in the 3-dimensional domain in figures (22), (23) and (24) respectively at time  $T=0.05$  and  $T=0.5$ . We have also shown the solution  $v$  in 3-dimensional slice at different time levels in Fig 25.

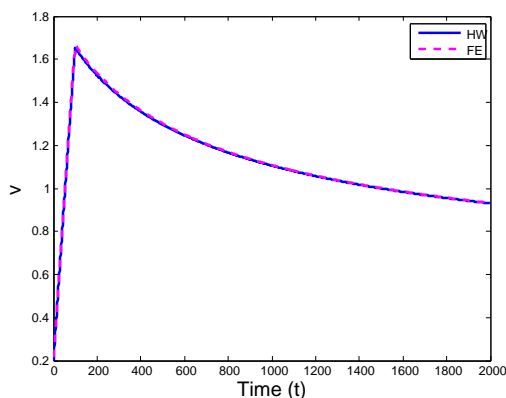


Fig. 21: **Comparison FE and HW solution  $v$  with  $J=4$  and  $T=1$  and  $dt = 10^{-3}$ .** at point (0.5312, 0.5312, 0.5312).

Next, we calculate the solution of the problem if the parameter  $\tau_{in}$  have jump discontinuity at some places in the domain, the corresponding function  $I_{ion}(v, w)$  will also be discontinuous, as shown in two dimensional case. The solution  $v$  corresponding to this  $\tau_{in}$  at the points (0.4062, 0.4062, 0.4062) and (0.2188, 0.2188, 0.2188), which are presented inside and outside the jump region respectively, of the domain is shown in Fig. 26. The smoothness of the solution with jump clearly shows that the Haar wavelets handle the jump discontinuity in the value of parameter  $\tau_{in}$ .

We also solved this problem using the linear finite element in space and implicit-explicit (IE) Euler method in time. Comparison of the computation time of finite element solution and the Haar wavelet solution for 3D level model in example 5 is given in Table 4. Clearly, from the table, the Haar wavelet method reduces the computational cost in comparison of FEM. Thus, it could be concluded that in higher dimension it is easy to use the Haar wavelet method to solve any problem even having the discontinuities.

	J	dt	FEM CPU time (sec)	HW CPU time (sec)
Example 5	2 (256 grid)	$10^{-2}$	73.7888	40.9545
	3 (1024 grid)	$10^{-2}$	571.902	143.249

Table 4: CPU time in 3D

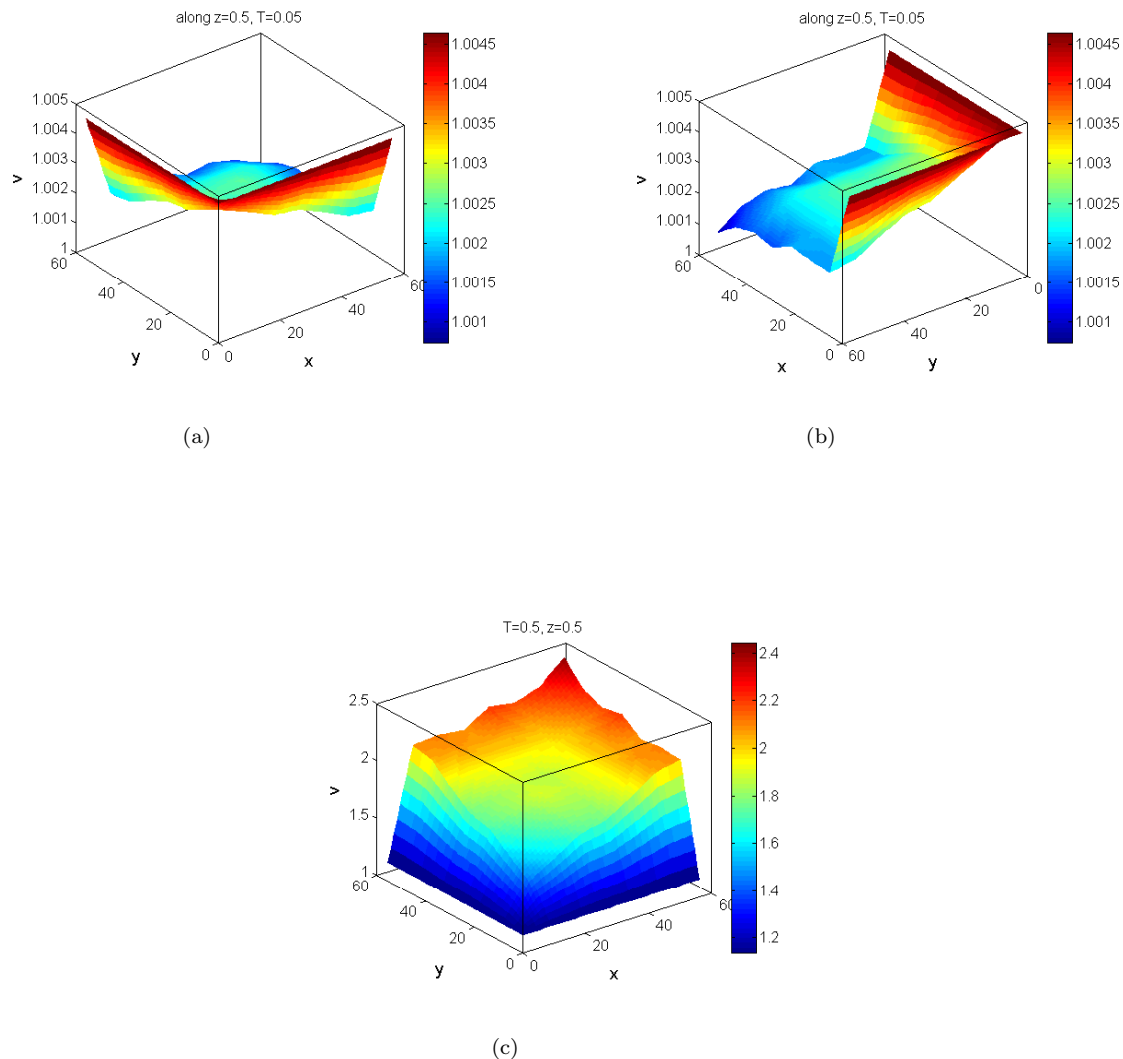


Fig. 22: HW solution along  $z=0.5$  at time, (a)  $T=0.05$ , (b)  $T=0.05$  (rotate view) (c)  $T=0.5$ .

J	cgs	bicg	bicgstab	gmres
$J = 5, dt = 10^{-3}$ (1D model)	7.629	6.70	8.345	5.2011
$J = 4, dt = 10^{-3}$ (2D model)	6.9015	6.8364	7.07158	6.4849
$J = 3, dt = 10^{-2}$ (3D model)	85.14	81.1456	83.8982	72.875

Table 5: CPU time with different solvers for 1D, 2D, and, 3D problems

## 6 Conclusion

A Haar Wavelet Method for a class of coupled non-linear PDE-ODEs system with jump discontinuities in model parameters or model coefficients has been proposed. The method is both simple and easy to implement in two and three dimensions. It is also computationally cost effective over linear finite element method. ILU-preconditioned GMRES Krylov solver accelerates the numerical solution convergence of the related linear system to required tolerances faster than other regular Krylov solvers. Convergence analysis has also been done to ensure the stability and accuracy. Numerical error reduces with the decrease in time step size or increase in resolution level. Model problems having single or multiple jump discontinuities in some parameters have been



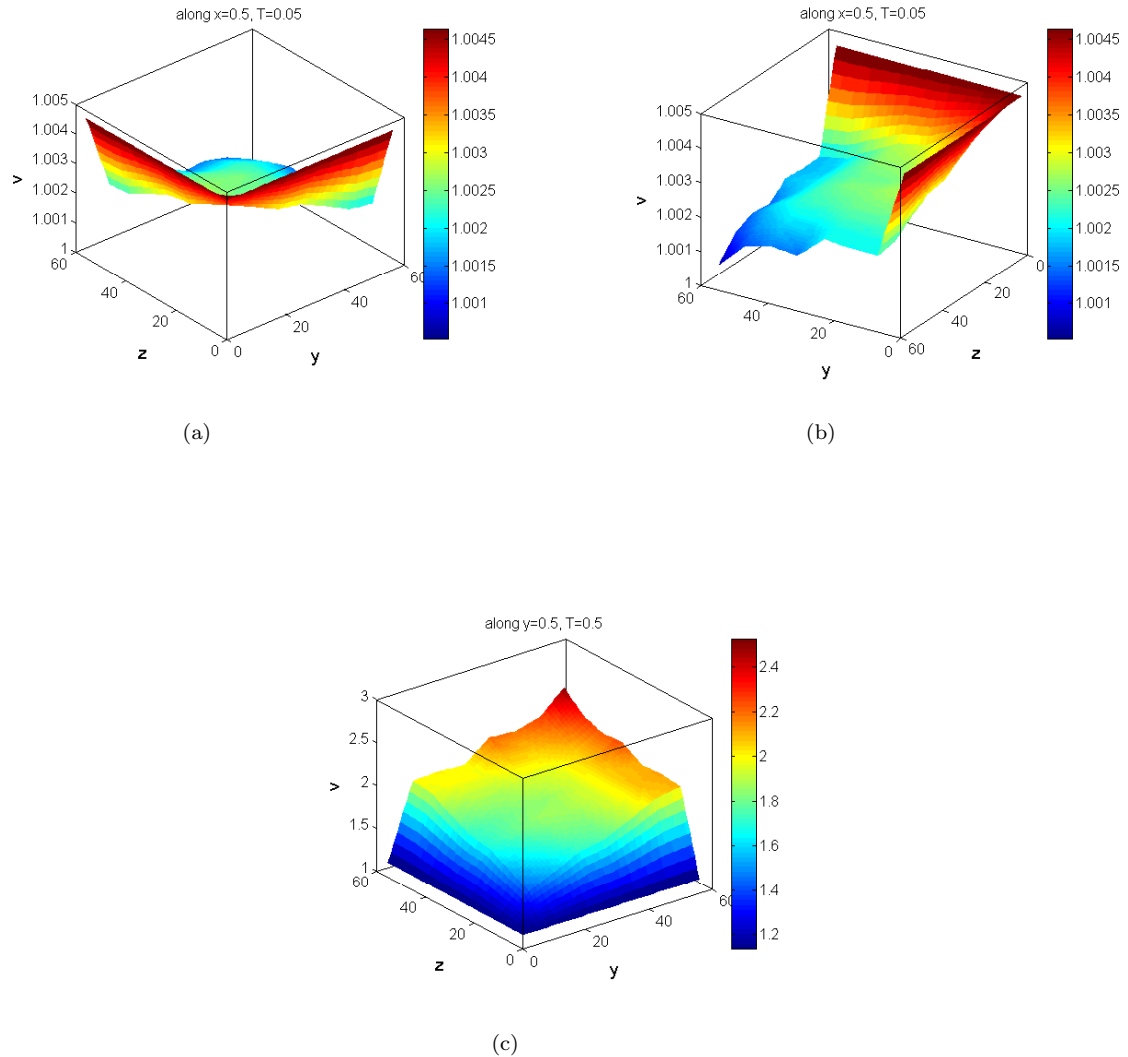


Fig. 23: HW solution along  $x=0.5$  at time, (a)  $T=0.05$ , (b)  $T=0.05$  (rotate view) (c)  $T=0.5$

successfully solved. Behavior of the solutions clearly indicated that Haar wavelets automatically handle such type of discontinuities. Problems with clinical relevance have also been successfully dealt with.

**Acknowledgements** Authors would to acknowledge SERB. Govt of India for funding the project (SERB/F/10196/2017-2018) on WGM for PDEs. We would also like to thank the DST for support through Inspire Fellowship, ID no. is IF130906.

## References

- Aziz I, Fayyaz M (2013) A new approach for numerical solution of integro-differential equations via haar wavelets. *International Journal of Computer Mathematics* 90(9):1971–1989
- Aziz I, Haq F, et al. (2010a) A comparative study of numerical integration based on haar wavelets and hybrid functions. *Computers & Mathematics with Applications* 59(6):2026–2036
- Aziz I, Šarler B, et al. (2010b) The numerical solution of second-order boundary-value problems by collocation method with the haar wavelets. *Mathematical and Computer Modelling* 52(9-10):1577–1590
- Aziz I, Khan W, et al. (2011) Quadrature rules for numerical integration based on haar wavelets and hybrid functions. *Computers & Mathematics with Applications* 61(9):2770–2781

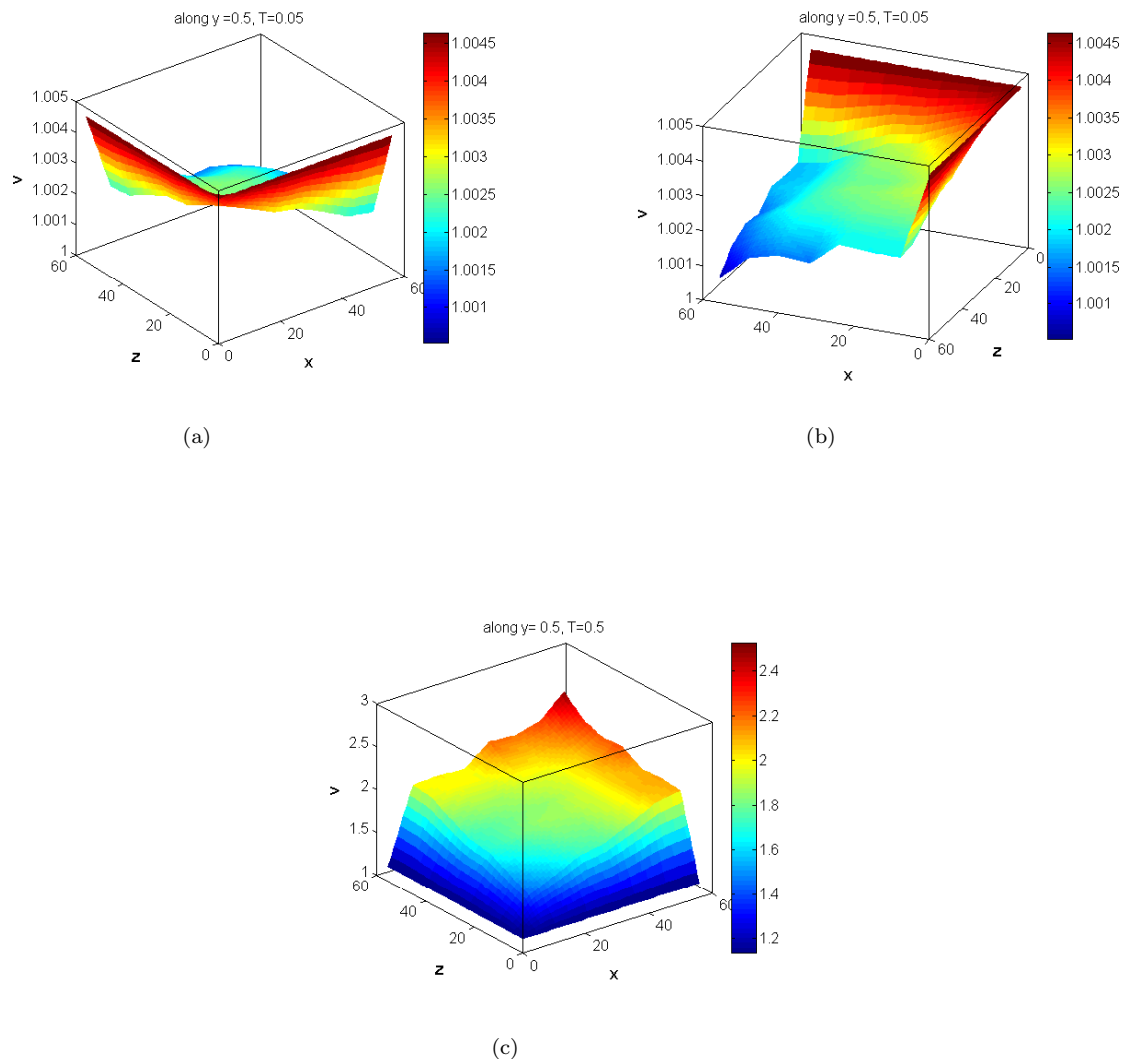


Fig. 24: HW solution along  $y=0.5$  at time, (a)  $T=0.05$ , (b)  $T=0.05$  (rotate view) (c)  $T=0.5$ .

- Aziz I, Khan W, et al. (2012) Numerical integration of multi-dimensional highly oscillatory, gentle oscillatory and non-oscillatory integrands based on wavelets and radial basis functions. *Engineering Analysis with Boundary Elements* 36(8):1284–1295
- Aziz I, Šarler B, et al. (2013a) Wavelets collocation methods for the numerical solution of elliptic boundary value problems. *Applied Mathematical Modelling* 37(3):676–694
- Aziz I, et al. (2013b) New algorithms for the numerical solution of nonlinear Fredholm and Volterra integral equations using Haar wavelets. *Journal of Computational and Applied Mathematics* 239:333–345
- Bernardi C, Verfürth R (2000) Adaptive finite element methods for elliptic equations with non-smooth coefficients. *Numerische Mathematik* 85(4):579–608
- Bonito A, Devaud D (2015) Adaptive finite element methods for the Stokes problem with discontinuous viscosity. *Mathematics of computation* 84(295):2137–2162
- Bonito A, DeVore RA, Nochetto RH (2013) Adaptive finite element methods for elliptic problems with discontinuous coefficients. *SIAM Journal on Numerical Analysis* 51(6):3106–3134
- Bourgault Y, Coudière Y, Pierre C (2006) Well-posedness of a parabolic problem based on a bidomain model for electrophysiological wave propagation. Preprint
- Bujurke N, Salimath C, Shiralashetti S (2008) Numerical solution of stiff systems from nonlinear dynamics using single-term Haar wavelet series. *Nonlinear Dynamics* 51(4):595–605

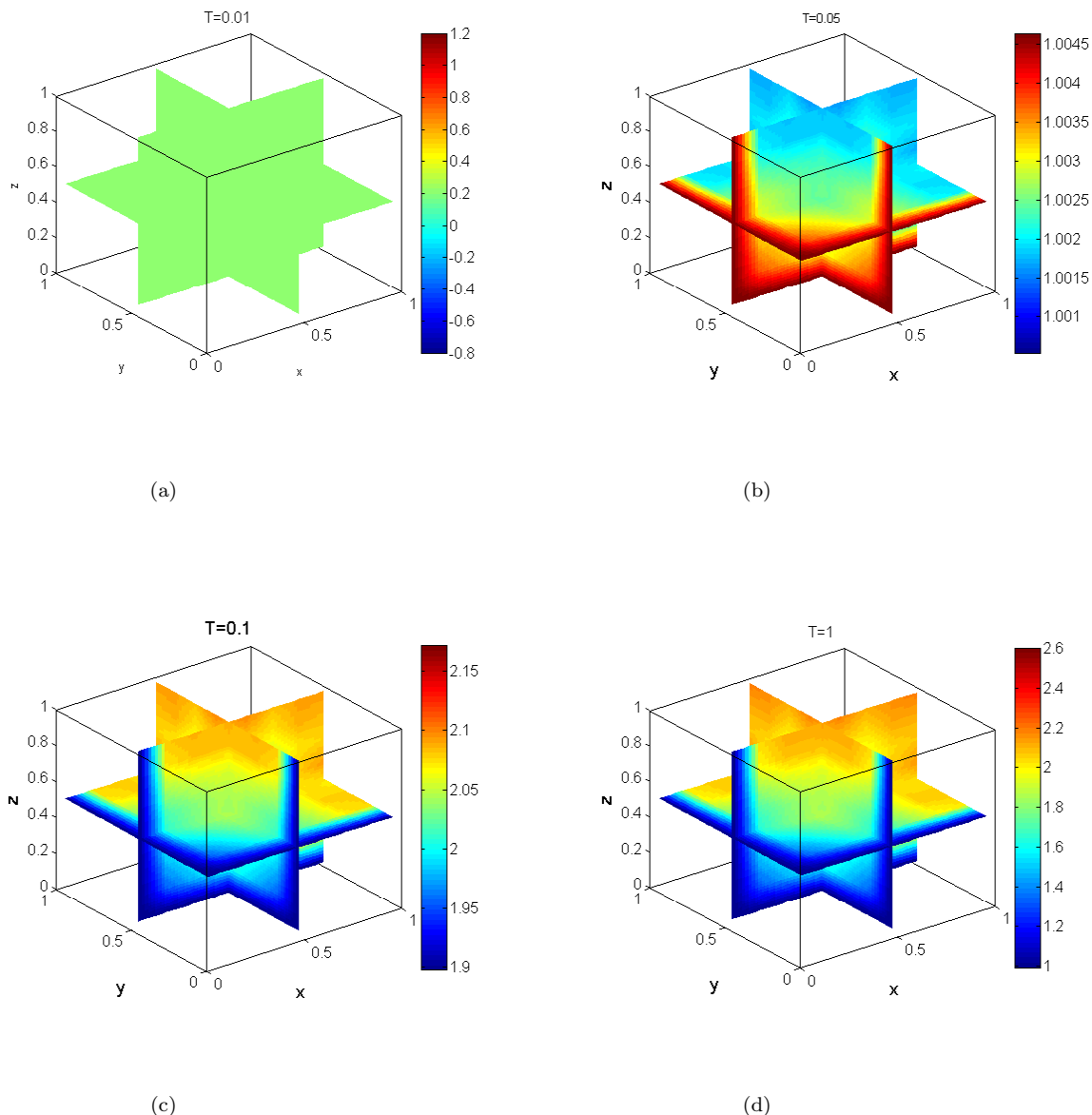


Fig. 25: HW solution in the Three dimensional domain at  $J=4$ ,  $dt = 10^{-2}$  at time, (a)  $T=0.01$ , (b)  $T=0.05$ , (c)  $T=0.1$ , (d)  $T=1$ .

- Chen C, Hsiao C (1997) Haar wavelet method for solving lumped and distributed-parameter systems. *IEE Proceedings-Control Theory and Applications* 144(1):87–94
- Comincioli V, Naldi G, Scapolla T (2000) A wavelet-based method for numerical solution of nonlinear evolution equations. *Applied numerical mathematics* 33(1-4):291–297
- Daafouz J, Tucsnak M, Valein J (2014) Nonlinear control of a coupled pde/ode system modeling a switched power converter with a transmission line. *Systems & Control Letters* 70:92–99
- Duarte CA, Oden JT (1996) An hp adaptive method using clouds. *Computer methods in applied mechanics and engineering* 139(1-4):237–262
- Fries TP, Belytschko T (2010) The extended/generalized finite element method: an overview of the method and its applications. *International Journal for Numerical Methods in Engineering* 84(3):253–304
- Göktepe S, Kuhl E (2010) Electromechanics of the heart: a unified approach to the strongly coupled excitation–contraction problem. *Computational Mechanics* 45(2-3):227–243

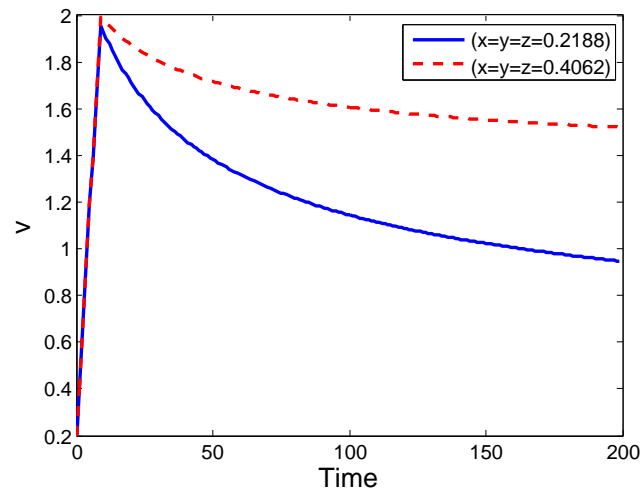


Fig. 26: Solution  $v$  with  $\tau_{in}$  parameter value having jump discontinuity.

- Hariharan G, Kannan K (2010) Haar wavelet method for solving some nonlinear parabolic equations. *Journal of mathematical chemistry* 48(4):1044–1061
- Hodgkin AL, Huxley AF (1952) A quantitative description of membrane current and its application to conduction and excitation in nerve. *The Journal of physiology* 117(4):500–544
- Keener J, Sneyd J (1998) *Mathematical physiology, Interdisciplinary Applied Mathematics*, vol 8. Springer-Verlag, New York
- Kestler S, Steih K, Urban K (2016) An efficient space-time adaptive wavelet galerkin method for time-periodic parabolic partial differential equations. *Mathematics of Computation* 85(299):1309–1333
- Lepik Ü (2007) Numerical solution of evolution equations by the haar wavelet method. *Applied Mathematics and Computation* 185(1):695–704
- Paolucci S, Zikoski ZJ, Grenga T (2014) Wamr: An adaptive wavelet method for the simulation of compressible reacting flow. part ii. the parallel algorithm. *Journal of Computational Physics* 272:842–864
- Plonsey R (1988) Bioelectric sources arising in excitable fibers (alza lecture). *Annals of biomedical engineering* 16(6):519–546
- Šarler B, Aziz I, et al. (2011) Haar wavelet collocation method for the numerical solution of boundary layer fluid flow problems. *International Journal of Thermal Sciences* 50(5):686–697
- Schneider K, Vasilyev OV (2010) Wavelet methods in computational fluid dynamics. *Annual review of fluid mechanics* 42:473–503
- Sepulveda NG, Roth BJ, Wikswo Jr JP (1989) Current injection into a two-dimensional anisotropic bidomain. *Biophysical journal* 55(5):987
- Shi Z, Cao Y (2012) Application of haar wavelet method to eigenvalue problems of high order differential equations. *Applied Mathematical Modelling* 36(9):4020–4026
- Singh I, Kumar S (2017) Wavelet methods for solving three-dimensional partial differential equations. *Math Sci (Springer)* 11(2):145–154, DOI 10.1007/s40096-017-0220-6, URL <https://doi.org/10.1007/s40096-017-0220-6>
- Vasilyev OV, Gerya TV, Yuen DA (2004) The application of multidimensional wavelets to unveiling multi-phase diagrams and in situ physical properties of rocks. *Earth and Planetary Science Letters* 223(1-2):49–64
- Veneroni M (2009) Reaction-diffusion systems for the macroscopic bidomain model of the cardiac electric field. *Nonlinear Anal Real World Appl* 10(2):849–868, DOI 10.1016/j.nonrwa.2007.11.008, URL <https://doi.org/10.1016/j.nonrwa.2007.11.008>

- 
- Vynnycky M, Mitchell S (2013) On the accuracy of a finite-difference method for parabolic partial differential equations with discontinuous boundary conditions. *Numerical Heat Transfer, Part B: Fundamentals* 64(4):275–292
- Wu JL (2009) A wavelet operational method for solving fractional partial differential equations numerically. *Applied Mathematics and Computation* 214(1):31–40